Westinghouse Non-Proprietary Class 3

WCAP-15949-NP
Revision 1

July 2003

AP1000 Reactor Internals Flow-Induced Vibration Assessment Program

WCAP-15949-NP
Revision 1

AP1000 Reactor Internals Flow-Induced Vibration Assessment Program

M. D. Snyder
S. Yonemoto (MHI)
R. E. Schwirian
D. A. Altman
E. A. Eggleston
N. R. Singleton

July 2003

AP1000 Document: APP-MI01-GER-001, Revision 1

Westinghouse Electric Company LLC
P.O. Box 355
Pittsburgh, PA 15230-0355

TABLE OF CONTENTS

TABLE OF CONTENTS (cont.)

LIST OF TABLES

LIST OF TABLES (cont.)

LIST OF FIGURES

LIST OF FIGURES (cont.)

1 INTRODUCTION

With respect to the reactor internals preoperational test program, the first AP1000 plant reactor vessel internals are classified as prototype as defined in the U.S. Nuclear Regulatory Commission (NRC) Regulatory Guide 1.20, Revision 2. AP1000 reactor vessel internals do not represent a first-of-a-kind or unique design based on the general arrangement, design, size, or operating conditions. The units referenced as supporting the AP1000 reactor vessel internals design features and configuration have successfully completed vibration assessment programs, including vibration measurement programs. These units have subsequently demonstrated extended satisfactory inservice operation. Additional background on the Westinghouse position with regard to NRC Regulatory Guide 1.20 is provided in Westinghouse Nuclear Safety Position Papers (References 1-2 and 1-3).

The vibration assessment approach for the AP1000 is believed to meet the intent of NRC Regulatory Guide 1.20 and is similar to the approach taken by Westinghouse on previous plants. Westinghouse performed a similar vibration assessment in support of the AP600 Design Certification. The AP600 vibration assessment was documented in Reference 1-4. This report provides a similar format and content as was provided for the AP600 assessment.

The purpose of this AP1000 reactor internals vibration assessment program is to demonstrate structural adequacy with respect to flow- and pump- induced vibrations. Estimates of flow-induced vibration levels and forces (or relative values) of the AP1000 plant are made on the basis of scale model tests, tests on prototype reactors, and results of analytical calculations. Based on this information, the vibratory behavior of the reactor internals is well characterized and the vibration amplitudes are sufficiently low for structural adequacy of the components.

The H. B. Robinson no. 2 plant has historically been established as the prototype design for three-loop plant internals and was instrumented and tested during hot functional testing. The test and analysis results of the three-loop configuration of Reference 1-3 demonstrate that the vibration levels of the reactor internals components are low and that the vibrations are adequately characterized to ensure structural integrity. These results are further augmented by References 1-5, 1-6, 1-7, and 1-8 to address the effects of successive hardware improvements in Westinghouse designs, which are discussed in the following sections.

The AP1000 reactor internals are generally similar to subsequent three-loop, 12- and 14-foot core designs (specifically Doel 3 and Doel 4), which have incorporated these improvements, and on which instrumented plant test programs have been completed. The dimensions of the AP1000 core barrel wall thickness and reactor vessel to core barrel downcomer annulus are similar to those of Doel 3 and Doel 4. The AP1000 guide tube and support column designs are the same as the designs used in Doel 3 and Doel 4. The upper internals components vibration responses were measured at Doel 3 (Reference 1-9), and the lower internals were measured at Doel 4 (Reference 1-10).

The total reactor mechanical design flow rates in these instrumented tests were approximately [ ]b(1) and [ ]b as compared to the AP1000 value of [ ]b mechanical design flow. Table 1-1 lists the ratios of the AP1000 to Doel 4 plant velocities at various locations based on flow rates of [ ]b for Doel 4 and 327,600 gpm for the AP1000 design. The tabulated velocities show similar values for the AP1000 and Doel 4 reactors with the exception of the inlet nozzle (AP1000 is 18 percent higher) and the downcomer AP1000 is 13 percent lower. Corresponding Doel 3 ratios are ~2.5 percent higher using [ ]b for the mechanical design flow rate of Doel 3.

The AP1000 internals have two component changes:

- The baffle plates and formers have been replaced by a core shroud, which rests on and is bolted to the lower core support plate.

- The structures below the lower core support plate have been modified consistent with the routing of the in-core instrumentation cables through the upper head and to accommodate a larger plate to suppress vortices in the core inlet plenum.

The preoperational test program of the first AP1000 plant includes a vibration measurement program and a pre- and post-hot functional inspection program. This program satisfies the guidelines for a NRC Regulatory Guide 1.20 Prototype Category plant. The first and all subsequent to AP1000 reactors will be subject to the pre- and post-hot functional visual inspection program. The program for plants subsequent to the first plant satisfies the guidelines for a Non-Prototype Category IV plant. This approach was also followed in the AP600 Design Certification.

Table 1-1 Reactor Internals Coolant Flow Velocity Ratios

Location	AP1000/Doel 4
Inlet nozzle at reactor vessel inside diameter	1.18
Downcomer (reactor vessel to core barrel annulus)	0.87
Lower plenum (downcomer exit)	1.01
Reactor core	1.00
Outlet nozzle at core barrel inside diameter	1.04

1. "[ ]" indicates that the enclosed data is proprietary. The superscripts are defined as follows:
   "a" – Information reveals the distinguishing aspects of a process or component, structure, tool, method, etc.
   "b" – Information consists of supporting data relative to a process or component, structure, tool, method, etc.
   "c" – Information, if used by a competitor, would reduce competitor's expenditure of resources or improve the competitor's advantage in the design, manufacture, etc., of a similar product.

2 SUMMARY

The AP1000 reactor internals represent an evolutionary change from the original Westinghouse designs for the prototype two-, three-, and four-loop plants.

The AP1000 reactor and internals are dimensionally similar to previous Westinghouse three-loop plants, and therefore, the vibratory behavior of its major structural components will be similar. A comparison of flow rates for various plants is included in section 4, which shows the AP1000 flow rate to be slightly higher (~4 percent) than the most recent Westinghouse three-loop plants.

The AP1000 reactor internals incorporate many design features introduced in other Westinghouse plants. The inverted top hat (or upper head injection [UHI] style) upper internals was instrumented at Sequoyah Unit 1, the lead UHI four-loop plant. This style upper internals – with its 17x17 guide tubes and solid, rather than slotted, upper support columns – has become the standard design for subsequent three- and four-loop plants. These features were also incorporated into the replacement two-loop upper internals assemblies provided for Prairie Island Units 1 and 2.

The lower internals have also undergone changes. The thermal shield or neutron panels have been removed from the core barrel. That results in a decreased flow velocity in the reactor vessel to core barrel downcomer annulus. The original lower core and support plates have been combined into a single plate, which was introduced in the three- and four-loop XL (extended length fuel) plants. Lower internals with one or both of these features (Paluel 1) were instrumented in preoperational vibration measurement programs at Doel 4 and Paluel 1, respectively.

The evolutionary changes introduced in previous Westinghouse plants have demonstrated their adequacy through a combination of plant measurement programs and successful operation over several fuel cycles. In addition, all Westinghouse units have undergone a thorough visual inspection of the reactor vessel internals before and after hot functional testing. These inspections have not indicated any abnormal wear, impacting, or excessive vibration displacements. The assessment in this report indicates that flow-induced vibrations of the AP1000 internals are adequately low.

The changes that are unique to the AP1000 reactor internals will be instrumented for a Preoperational Vibration Measurement Program as discussed in section 7. The results of the prototype AP1000 test program will further demonstrate the adequacy of the reactor internals design.

3 DESIGN DIFFERENCES AND RELATIONSHIP TO FLOW-INDUCED VIBRATIONS

This section provides a discussion of the evolution of the design changes introduced in the AP1000 internals. The discussion focuses on the design changes to the H. B. Robinson internals and provides a discussion of their possible relationship to flow-induced vibrations. As mentioned in section 1, the Westinghouse three-loop prototype plant is H. B. Robinson. Subsequent structural differences include modifications resulting from the use of 17x17 fuel, the removal of the annular thermal shield, and the change to the (UHI style) inverted top hat support structure configuration. The effects of these changes were determined by instrumented test programs at Trojan, Sequoyah 1, Doel 3, and Doel 4. The primary changes from the Doel 3 and Doel 4 designs are the addition of a vortex suppression plate beneath the lower core plate, the inclusion of a core shroud within the core barrel, and the change from bottom- to top-mounted in-core instrumentation.

Many features of the AP1000 reactor design are the same as those of designs now in operation. For example, compared to a 3XL design, the number of fuel assemblies, and the core barrel inside diameter and outside diameter are the same; and the reactor vessel diameters are similar. In addition, many of these design features have been incorporated in the AP600 design. The differences between an AP1000 reactor and a 3XL reactor are primarily as follows:

- There is increased core barrel length and consequential lowering of the lower support plate into the lower head of the reactor vessel.
- The baffle-former structure is replaced with a core shroud. The core shroud is similar to those in operation in Westinghouse/Combustion Engineering nuclear plants.
- The neutron pads attached to the outer wall of the core barrel in the 3XL design are deleted.
- There is slightly higher (roughly 4 percent) reactor flow rate.
- Reactor vessel head-mounted instrumentation replaces bottom-mounted instrumentation.
- The AP1000 design has additional guide tubes and upper support columns.
- The AP1000 reactor vessel overall length is slightly less than the overall length of the 3XL vessel.
- The AP1000 reactor vessel ID is 0.4 inches (10.2 mm) smaller than that of the 3XL design.
- The AP1000 design has four inlet nozzles and two outlet nozzles; the inlet nozzle centerlines are at a higher elevation than the centerlines of the outlet nozzles. The 3XL design has three inlet nozzles and three outlet nozzles all having centerlines at the same elevation.
- The projected flow area of an AP1000 outlet nozzle is larger than that of the 3XL.

- The core barrel lower restraint keys are 45° from the cardinal axes in the AP1000 design as opposed to being on the axes in the 3XL design.

The design similarities, the design differences, and their relationships to the flow-induced vibrational characteristics are discussed in the following sections.

3.1 LOWER INTERNALS ASSEMBLY

The AP1000 lower internals are similar to the 3XL design (Figure 3-1) for which a preoperational vibration measurement program was conducted at Doel 4. The diameter and thickness of the core barrel wall are almost identical between these two plants. The 3XL and AP1000 lower internals both have the single combined lower core support plate.

Design changes incorporated between the AP1000 and the 3XL lower internals assembly designs include:

- Core barrel length has been increased 11.2 inches.
- Thermal shield and/or neutron pads have been eliminated (same as AP600).
- Baffle former assembly has been replaced with a core shroud.
- Guide columns for the in-core bottom-mounted instrumentation have been deleted (same as AP600).
- Vortex suppression plate and support columns have been incorporated (same as AP600).

As indicated above, some of these design changes were also incorporated in the AP600 design. In addition, the baffle former assembly was replaced in the AP600 design with a radial reflector. The radial reflector was not included in the AP1000 design, and instead, a core shroud design has been incorporated.

Results from Indian Point and Trojan (Reference 1-4), as well as scale model test results (Reference 1-5), show that core barrel vibration of plants with neutron shielding pads is less than that of plants with thermal shields. The removal of the neutron pads in the AP1000 design further reduces flow velocities in the reactor vessel core barrel downcomer annulus by increasing the flow area. In addition, core barrel responses were measured in a plant vibration measurement program at Paluel (Reference 3-1), which is a four-loop plant without neutron pads. These responses are lower than those for four-loop neutron pad core barrels measured at Trojan 1 for the same flow rate.

The longer core barrel and the loss of the stiffening effects of the baffle/former structure tend to increase the vibration responses of the lower internals. These factors and the higher flow rate of the AP1000 design result in a slightly higher calculated radial vibration root-mean-square (RMS) displacement at the lower core support elevation of the core barrel. This is discussed in detail in subsection 5.3.2.

Removal of the baffle formers also reduces the core barrel shell mode stiffnesses. The reduced stiffness combined with a potential for higher added water mass in the barrel-core shroud annulus, however, will tend to increase the vibratory response levels of the core barrel shell modes relative to the 3XL design. The AP1000 core barrel shell mode responses are discussed in subsection 5.3.2.

The core shroud is basically a cylindrical structure, which rests on and is bolted to the lower core support plate. Restraint of the upper end of the core shroud is provided by four pins with small tangential gaps relative to clevices that are attached to the core barrel. The AP1000 core shroud is similar to the designs of previous Westinghouse/Combustion Engineering designs, including the System 80 design, and more recent designs supplied in Korea.

The change to top-mounted in-core instrumentation has simplified the structure beneath the lower support plate. Although the secondary core support (energy absorber) has been retained, the guide columns and tie plates associated with the bottom-mounted in-core instrumentation have been eliminated.

A vortex suppression plate (Figure 3-2) has been added. This plate consists of two annular rings connected by four spokes. The inner ring of the vortex suppression plate is supported by four columns, which also form part of the secondary core support. The outer annular ring is suspended beneath the lower core plate by eight equally spaced butt columns. The vortex suppression plate has been shown to suppress the formation of standing vortices in the core inlet plenum in laboratory testing performed for the AP600 design (Reference 3-2). The response of this structure will also be measured during the AP1000 reactor internals preoperational measurement program.

3.2 UPPER INTERNALS ASSEMBLY

Figure 3-3 shows the upper internals for the three-loop prototype, Doel 3/Doel 4, and AP1000. The upper support plate for the guide tubes and support columns becomes a simple structure in the form of an inverted top hat as shown in Figure 3-4. It consists of a flange, a skirt, and a thick base plate connected by two circumferential welds. The original design included a thinner plate stiffened by a system of ribs attached by corner-welding (deep beam structure). The change to the new design results in shorter and stronger (17x17 AS) guide tubes, which are less susceptible to flow-induced vibrations. The AP1000 guide tube design has stainless steel support pins and a guide plate to enclosure attachments by pins instead of card tabs. (This guide tube design is installed in the Sizewell B reactor.)

The AP1000 inverted top hat (UHI style) upper support structure is the same design as in the Doel 3 and Doel 4 upper internals. Therefore, the same general vibration behavior is expected. The components of the upper internals are excited by turbulent forces due to axial and cross flow in the upper plenum and by pump-related excitations (References 1-5 and 1-8).

The upper support assembly skirt (Figure 3-4) is approximately 10 inches longer than the previous three-loop internals inverted top hat designs, such as Doel 3 and Doel 4. However, the structural characteristics are not expected to change significantly relative to those observed at Doel 3 and Doel 4 since the support plate, flange, and skirt thicknesses and diameters are the same.

The AP1000 upper internals assembly has different numbers of guide tubes and support columns as compared to the Doel 3 and Doel 4 plants (Figure 3-4). The AP1000 design has a total of 69 guide tubes versus 53 and 57 in Doel 3 and Doel 4, respectively. In addition, the AP1000 design has 42 support columns rather than the 40 used in the Doel 3 and Doel 4 plants. These differences are expected to have little effect on the upper internals responses measured in the 3XL 1/7 scale model and Doel 3 plant preoperational measurement program. Since the guide tubes and support columns dominantly respond as individual beams restrained by the upper support plate and upper core plate at their top and bottom ends

respectively, additional numbers of these components will not alter the dynamic characteristics of these components. Mean loads and vibratory amplitudes are calculated for the components of the AP1000 array using a calculation method based on reference plant test data as described in subsection 6.3.3 of this report.

The AP1000 upper internals include an extension to the support columns above the upper support plate that is part of the new top-mounted in-core instrumentation system. This tubular component is mounted to the top surface of the upper support plate, and the upper end fits within a counterbore provided in the head penetration tube (Figure 3-3). Vibration of the upper support column extensions resulting from the [ ]^{b,c} percent core bypass flow is expected to result in high cycle fatigue stresses within code allowable limits. The bypass flow is directed into the reactor vessel head plenum through the head cooling nozzles, which are located near the reactor vessel head inner diameter. The bypass flow is directed vertically upward and tends to follow the head inner surface. This nozzle arrangement, in combination with the lateral separation from the nearest support column extension, prevents direct impingement of the flow on the support column extension.

a,c

Figure 3-1 Design Differences in Lower Internals

Note – All columns are 5-inch diameter.

Figure 3-2 Vortex Suppression Plate

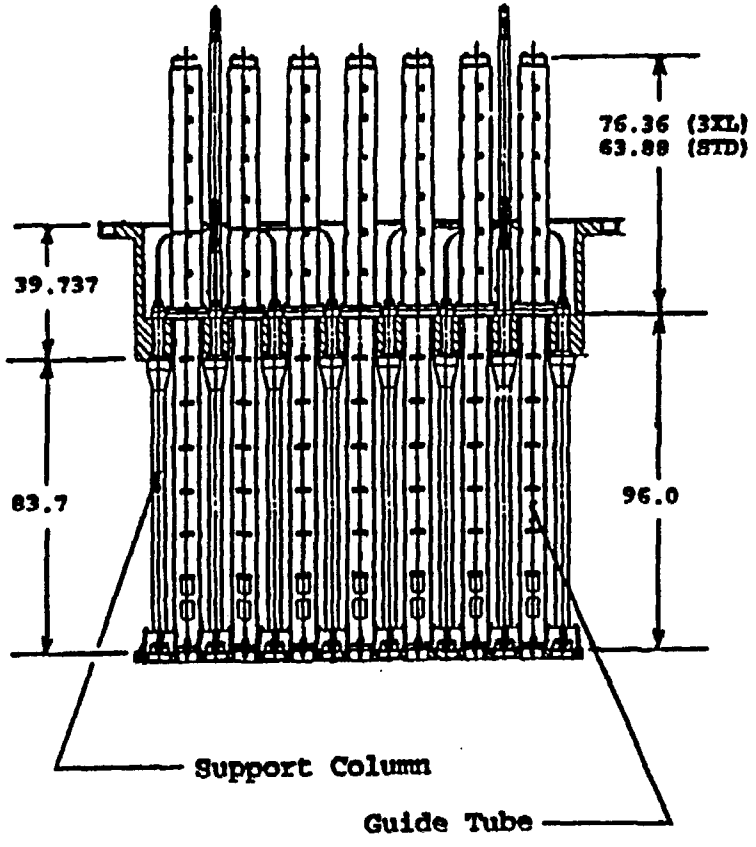

Doel 3/Doel 4

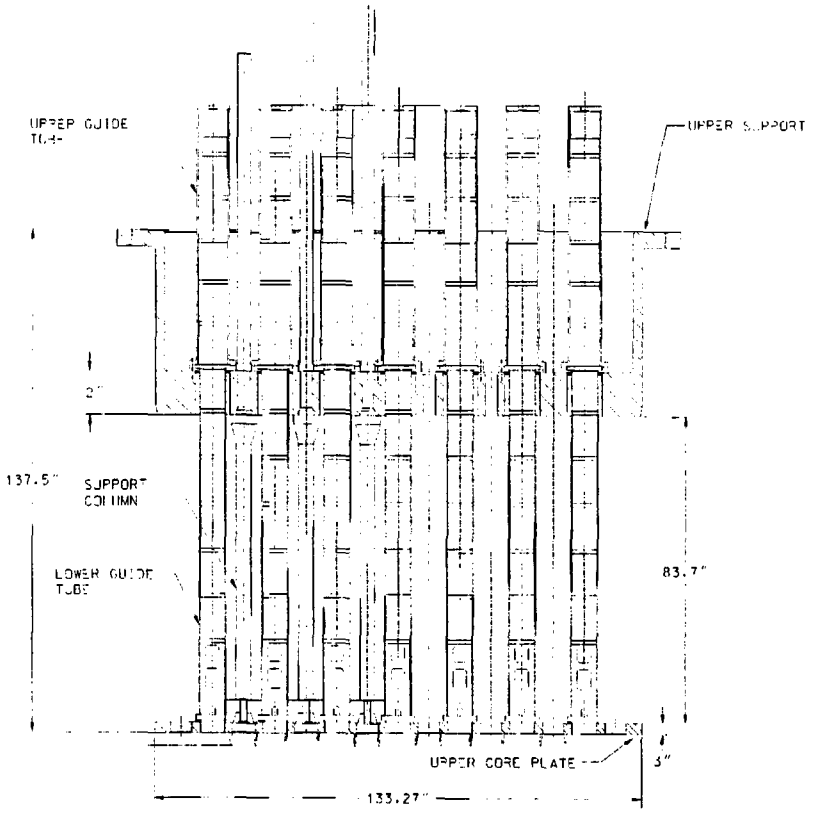

AP1000

Figure 3-3 Upper Internals (Elevation)

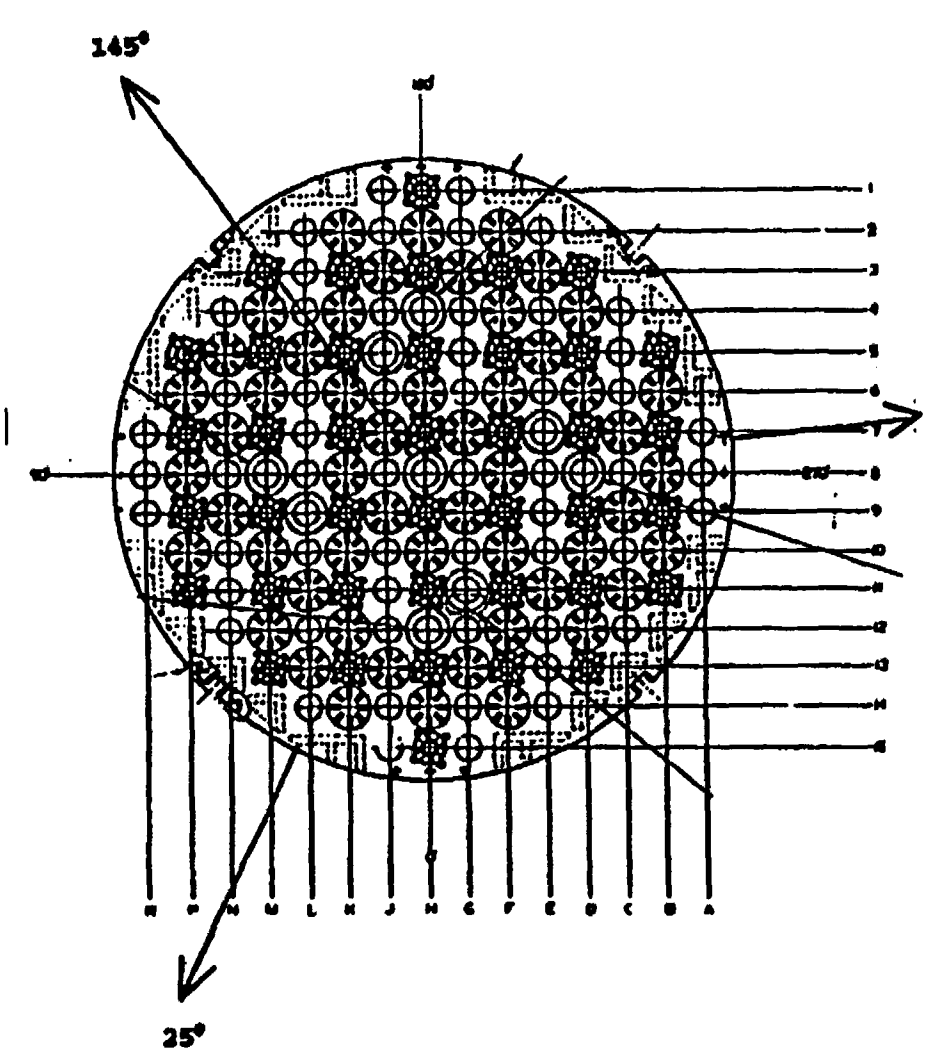

Doel 3/Doel 4

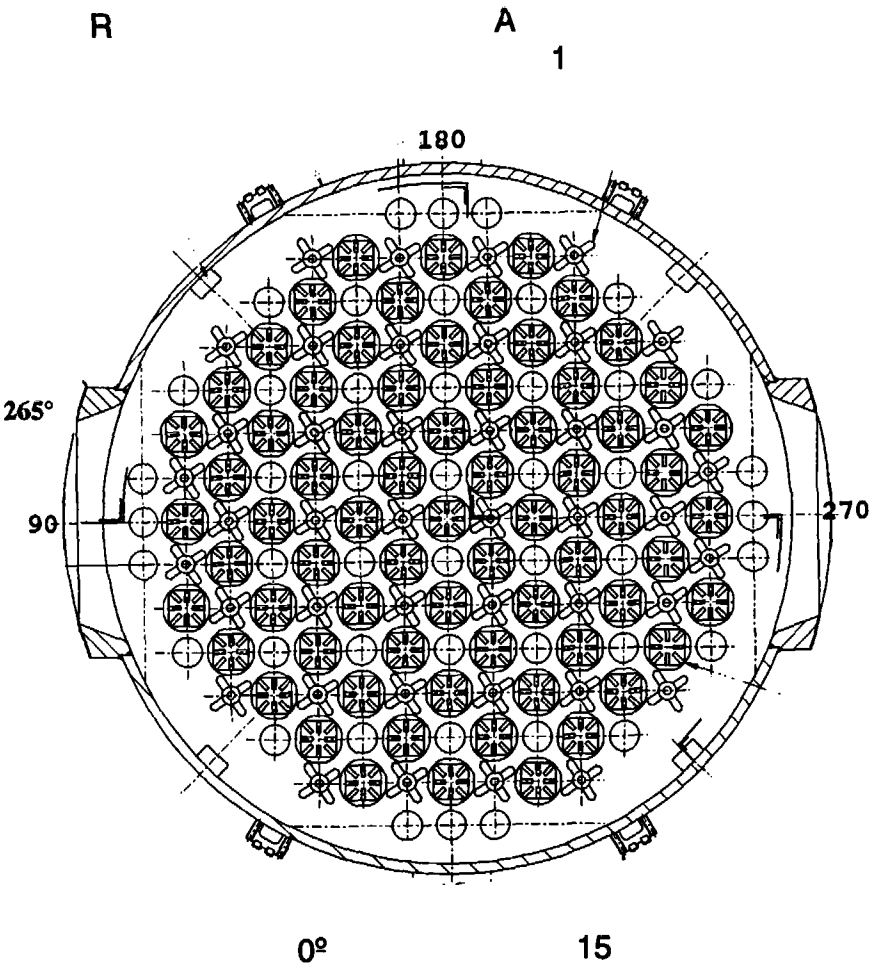

AP1000

Figure 3-4 Upper Internals (Cross Section)

4 WESTINGHOUSE EXPERIENCE: SCALE MODEL AND PLANT TESTS

4.1 GENERAL

The program developed by Westinghouse to demonstrate and support the adequacy of reactor internals due to flow-induced vibrations includes the following:

- Analytical studies to determine natural frequencies, mode shapes, vibration amplitudes, and stresses
- Scale model tests
- Vibration measurement tests on prototype reactors
- Pre- and post-hot functional examination on each plant

This program has been applied to one-, two-, three-, and four-loop reactors and has shown that the behavior of the four sizes is similar. Therefore, the results obtained have complemented one another and made possible a better understanding of the flow-induced vibration phenomena.

This section provides a summary of the scale model test programs and in-plant test programs used to support the AP1000 reactor internals vibration assessment. As the AP1000 reactor internals represent an evolutionary step in the design of reactor internals, results of these test programs can be factored into the design and analysis of the AP1000 reactor internals. Table 4-1 provides a summary of these test programs used to support the AP1000 reactor internals vibration assessment.

Westinghouse has developed detailed computational fluid dynamic (CFD) and finite-element models of both the 3XL and the AP1000 reactor vessel and internals designs as discussed in sections 5 and 6 of this report. The 3XL finite-element model is used to calculate vibratory-induced deflections, and the calculated values are compared to applicable plant test data taken during the Doel 4 hot functional testing. The finite-element modeling techniques are refined to accurately predict the Doel 4 test results, and these modeling techniques are applied in the AP1000 model. The CFD model was used to determine the steady-state flow loads on the upper internals components.

Table 4-1 is a summary of these tests. It provides a background for the information that is used to support the assessment of the AP1000 reactor internals vibrations.

4.2 TEST RESULTS APPLICABLE TO LOWER INTERNALS

Table 4-2 summarizes information on core barrel cantilever beam mode (with no lower contact at the restraints) vibration amplitudes. These data are discussed in the following paragraphs.

- Scale model tests (Reference 1-5) as well as prototype tests (Reference 1-4) indicate that designs with circular thermal shields have higher beam mode vibration amplitudes than those with

neutron pads. Based on scale model test data, the H. B. Robinson core barrel vibration amplitude is estimated to be [ ]^{b} mils rms.

- The vibrations of three-loop neutron pad core barrels have been measured in plant tests. Estimates of the vibration amplitude from scale model tests are similar to or greater than the value measured during the Tricastin plant test. This and other scale model-prototype comparisons provide confidence in the core barrel vibration estimates from scale model data.

- The 4XL scale model estimates for Paluel vibration amplitudes are identical to the plant measurements. This indicates that removal of the neutron pads does not significantly affect the vibration amplitude. The slightly higher natural frequency resulting from reduced hydrodynamic mass and structural mass, and the lower downcomer velocity resulting from increased downcomer area (~[ ]^{a,b} in three-loop plants) would tend to reduce the excitation of the core barrel as a result of removing the neutron pads.

A summary of measured core barrel natural frequencies for past reactor vessel internals designs is provided in Table 4-2. Similar natural frequencies are shown for all data. The differences are primarily due to differences in the hydrodynamic mass generated in the downcomer annulus. Calculations performed for the AP1000 design are discussed in section 6 of this report and demonstrated that the AP1000 core barrel natural frequency is similar to that of past plants, and that the estimated amplitude is small, and within the range of existing designs.

The core barrel shell mode measured responses from the 3XL scale model and from the plant test data (References 1-9 and 4-1) are summarized in Tables 4-3 and 4-4. These results are used in section 7 to estimate the AP1000 shell mode responses.

4.3 TEST DATA APPLICABLE TO UPPER INTERNALS

4.3.1 General

As mentioned in section 3.2, the AP1000 inverted top hat upper support structure is the same design as the Doel 3 and Doel 4 upper internals, and therefore, the same general vibrational behavior is expected. Since the flow turbulences are generated by cross flows that converge on outlet nozzles, the more highly loaded components (such as upper support columns and guide tubes) lie within the vicinity of the outlet nozzles. The AP1000 outlet nozzle velocity is approximately 4 percent higher than the velocity of the previously measured three-loop reactor. Considering the higher velocity and the larger diameter outlet nozzle, the corresponding upper internals flow loads are expected to be slightly higher.

4.3.2 Upper Support Plate

A vertically sensitive accelerometer was mounted to detect vibration at the center of the upper support plate, and a vertically sensitive strain gage was mounted on the inner wall of the skirt in Doel 4 hot functional testing. The data from these transducers are used as part of the 3XL reference data in section 5.2 of this report.

4.3.3 Guide Tubes and Support Columns

In section 6.2, the mean flow-induced loads on the most highly loaded components during the previously instrumented (Doel 3) and 3XL 1/7 scale model tests are calculated using computational fluid dynamics (CFD) analyses. The mean flow loads have been shown to be related to vibration amplitude using 1/7 scale model data. In the following, 1/7 scale model data are compared to plant data for three-loop configurations, showing the adequacy of the 1/7 scale model for prediction of upper internals component vibrations.

The 3XL 1/7 scale model tests were also used as reference data for mean loads to determine the guide tube and support column vibration spectrum (strain versus frequency). The scale model test guide tubes and support columns were instrumented with axial strain gages, and the test data was used to determine the vibration spectrum.

Tables 4-5 through 4-7 show the comparisons between the 3XL 1/7-scale model test data and the Doel 3 plant data. Tables 4-6 and 4-7 indicate that the 1/7 scale model of the 3XL plant overpredicts the response of the upper support columns and guide tubes when compared to the Doel 3 plant test data. Guide tube mean flow and vibration measurements have also been made in a two-loop plant (Reference 4-2). The results showed behavior similar to guide tubes measured in three- and four-loop plants.

The mean flow-induced loads are also calculated for the AP1000 reactor using the same CFD analysis techniques. Comparison of the AP1000 calculated frequencies and discussed in section 6 of this report.

Table 4-1 Test Information on Flow-Induced Vibration of Reactor Internals

Test	Purpose/Main Observations
Four-loop thermal shield 1/24 scale model	• Lower internals flow-induced vibration • Comparison with prototype data
Three-loop thermal shield 1/22 scale model	• Lower internals flow-induced model test • Similar to four-loop internals vibration
Indian Point plant test (four-loop prototype)	• Verified adequacy of internals • Verified accuracy of scale models and analyses • Verified use of hot functional test (no core) for vibration assessment • Provided data for improved predictions and forcing functions
H. B. Robinson (three-loop prototype)	• Showed behavior similar to four-loop • Provided data for improved predictions
Four-loop neutron pad 1/24 scale model test	• Showed neutron pad internals have behavior similar to thermal shield internals and vibration levels to be significantly lower
Three-loop neutron pad 1/22 scale model test	• (Same as above) • Showed three- and four-loop internals vibration similar
R. E. Ginna (two-loop prototype)	• Two-loop internals vibration similar to three- and four-loop internals vibrations
Trojan 1 plant test (neutron pad prototype)	• Additional verification of scale model and analysis predictions • Verified adequacy of 17x17 guide tubes and neutron pad designs • Verified reduced vibration levels of neutron pad and 17x17 design changes
1/7 scale UHI internals test	• Flow-induced vibration of solid support columns and 17x17 guide tubes in the UHI array • Showed, with analysis, adequacy of guide tubes, and upper support columns
Sequoyah plant test (UHI prototype)	• Verified adequacy of support columns and guide tubes in inverted hat design. Additional verification of scale model testing technique.
4XL 1/7 scale model test	• Show similarity of UHI and 4XL upper internal responses

Table 4-1 (cont.) Test Information on Flow Induced Vibration of Reactor Internals

Test	Purpose/Main Observations
3XL 1/7 scale model test	• Vibration response of 3XL internals • Show similarity of three-loop, four-loop, and UHI upper internals vibratory behavior
Doel 3 plant test (French neutron pad prototype)	• Verified adequacy of three-loop inverted hat style upper internals
Doel 4 plant test (XL prototype)	• Verified adequacy of 3XL lower internals
Paluel plant test (French XL prototype)	• Verified lower response of core barrel without neutron pads

Table 4-2 Core Barrel Cantilever Beam Mode Response

Plant	Core Barrel Configuration	RMS Amplitude[1] (inches)	f_n (Hz)	Total Plant Flow Rate (gpm)	Data Source
H. B. Robinson	[		] b,c	268,500	1/22 scale model
Tricastin 1				[ ] b,c	Plant test 1/22 scale model 1/7 scale 3XL model
Doel 4				[ ] b,c	Plant test 1/22 scale model 1/7 scale 3XL model
South Texas (four-loop)				426,400	1/7 scale 4XL model
Paluel 1 (four-loop)	[		]	[ ] b,c	Plant test 1/7 Scale 4XL model (with neutron pads) 1/24 scale model (with neutron pads)

1. At an elevation near the lower end of the core barrel
2. Approximately at the elevation of the upper core plate

Table 4-3 Comparisons of Core Barrel Shell Mode Frequency (Hz)				
Shell Modes	1/22 Scale Model Three-Loop (312)	1/7 Scale Model 3XL (314)	Tricastin 1 Plant Test	Doel 4 Plant Test
n = 2 n = 2'	[			] b,c
n = 3 n = 3'				

Table 4-4 Comparison of Maximum Shell Mode Deformations			
Shell Modes	3XL Model Measurements	Tricastin 1 Measurements	Doel 4 Measurements
n = 2	[		] b,c
n = 3			

$\mu\varepsilon = 1.0 \times 10^{-6}$ in./in.

Table 4-5 3XL Scale Model Versus Doel 3 Upper Internals Frequencies		
Component	3XL 1/7 Scale Model	Doel 3 Plant Test
Lower guide tube		
0° - 180°	[	] b,c
90° - 270°		
Upper guide tube		
0° - 180°		
90° - 270°		
Support column		

a. From D-loop test of XL guide tube

Table 4-6 3XL Scale Model Versus Doel 3 Upper Internals Steady Flow Loads			
	3XL 1/7 Scale Model Test (LB_f)		Doel 3 Plant Test (LB_f)
Component	Adjusted for 3XL Flow, Hot Full Power	Adjusted for Doel 3 Flow, Hot Functional Test	Measured During Hot Functional
S.C. M-3	[		] b,c
S.C. B-7			
G.T. K-14			
G.T. B-8			
G.T. H-14			
G.T. B-6	[		]

1. CFD: Calculated from the CFX commercial program

S.C. = support column
G.T. = guide tube

Table 4-7 3XL Scale Model Versus Doel 3 Upper Internals Random Flow-Induced Vibratory Response			
	3XL 1/7 Scale Model Test (MILS)		Doel 3 Plant Test (MILS)
Component	Adjusted for 3XL Flow, Hot Full Power	Adjusted for Doel 3 Flow, Hot Functional Test	Measured During Hot Functional
S.C. M-3	[		] b,c
S.C. B-7			
S.C. B-7			
G.T. K-14			
G.T. B-8			
G.T. H-14			
G.T. B-6	[		]

1. Calculated in CN-EMT-02-141

S.C. = support column
G.T. = guide tube

5 AP1000 REACTOR SYSTEM VIBRATIONS AND FORCES

This section describes analyses that are used to estimate the vibratory forces due to the following:

- Broadband flow turbulence
- Turbulent excitation of the reactor coolant loop fundamental acoustic mode
- Reactor coolant pump (RCP) induced excitation
- Postulated vortex shedding

Section 5.1 describes the overall methodology used to apply these forces to the estimation of normal operation vibrational response of the AP1000. Section 5.2 describes the development for the four identified sources of excitation:

- Broadband turbulent forces are stationary random forces described by power spectral density functions (PSDs), which were estimated for the 3XL design using test data as discussed in section 4. Mathematical expressions for these PSDs were then developed for the 3XL plant by using CFD to define the parameters (velocity and vorticity) needed in these expressions at the locations where PSD data were taken. By adjusting these mathematical expressions to best fit the 3XL PSD data, these mathematical PSD expressions were optimized. The same basic expressions were then used to define PSDs in the AP1000 flow-induced vibration analysis by using CFD-calculated distributions of fluid velocity and vorticity for the AP1000 plant. Thus, the scaling from 3XL to AP1000 is performed in such a way that the fundamental aspects of the flow fields in the downcomer and lower plenum are taken into account. The details of this PSD development are discussed in subsection 5.2.1.

- The broadband turbulent forces described in subsection 5.2.1 are due to random turbulence generated in the region local to the internals on which the forces act. The 3XL data also shows evidence of some narrow-band turbulent excitation of the primary acoustic mode of the entire reactor coolant loop. Subsection 5.2.3 presents further description of this potential excitation and the basis for estimates of these forces in AP1000.

- Reactor coolant pump excitation produces narrow-band quasi-harmonic pressures at the pump rotating speed and multiples of the vane passing frequencies. As described in subsection 5.2.2, these pressures are estimated using an analytical model of the Reactor Coolant System (RCS).

- As described in subsection 5.2.4, vortex shedding forces are sinusoidal forces that are postulated to occur on structures in the lower plenum.

5.1 OUTLINE OF METHODOLOGY

The overall methodology of estimating vibrational forces and using these forces in predicting the response of the AP1000 plant is outlined in Figure 5-1. The figure shows three divisions to the analysis:

- As shown at the top of Figure 5-1, test and plant data were evaluated as described in section 3.

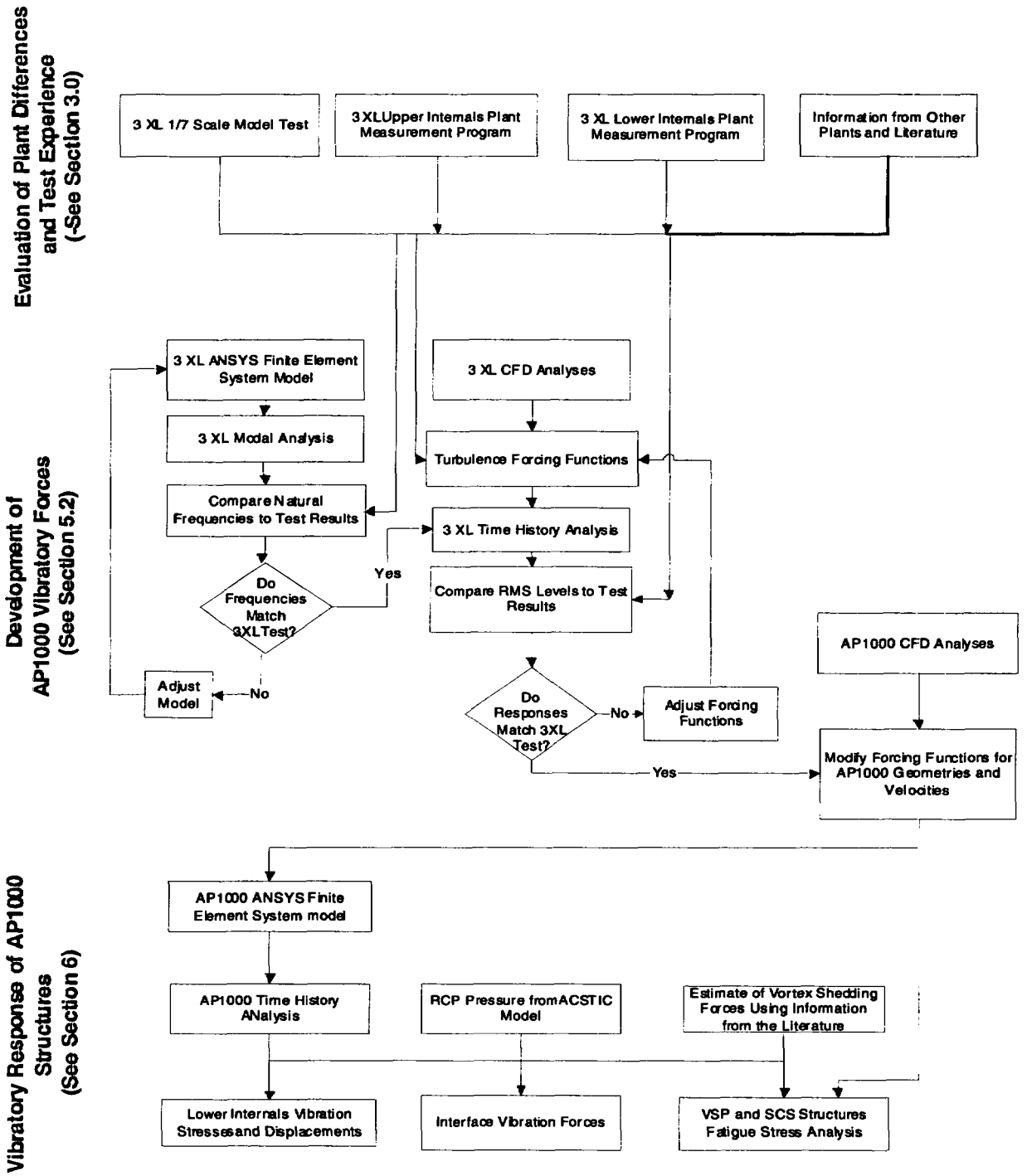

Figure 5-1 Analysis Methodology

- As shown at in the middle of Figure 5-1, broadband turbulence forces were assessed with the aid of a finite element models of the 3XL plant and CFD models of the AP1000 and 3XL plants. This is discussed in more detail in subsequent sections.

- As shown at in the bottom of Figure 5-1, vibratory response of the AP1000 structures was performed as described in section 6. The evaluations of the AP1000 response included the RCP excitation and vortex shedding forces developed using methodology described in subsections 5.2.2 and 5.2.4.

The development of broadband turbulent forces is emphasized in the middle section of Figure 5-1 since these are the predominant source of excitation. The methodology provided an analytical approach for evaluation of the effects of the design differences on the 3XL and AP1000 flow forces. Of particular significance, the CFD models provided a basis for assessing the effects of downcomer geometry, plenum geometry, and nozzle arrangements on turbulent forces.

The analysis proceeded as follows: A 3XL finite model was prepared and adjusted so that the frequencies predicted by the structural finite element model matched frequencies obtained from test data. Concurrently, a CFD analysis was performed of the 3XL inlet nozzle, downcomer, and lower plenum, and correlations were developed using the measured PSD test data and calculated flow field quantities. These correlations were used to define the turbulent force distributions acting in these regions. The turbulent forces were then applied to the 3XL finite element model and iteratively refined and adjusted to produce a conservative match to the 3XL structural response test data. Once the turbulent forces were refined to give conservative estimates of 3XL test results, a CFD analysis of the AP1000 inlet nozzles, downcomer, and lower plenum geometry was performed to define the flow field input to be used in the PSD correlations described previously. The turbulent forces thus generated were then applied to the AP1000 finite element model to determine its flow-induced vibration behavior.

5.2 DEVELOPMENT OF FORCING FUNCTIONS

5.2.1 Flow Turbulence

To perform a turbulence-induced vibration analysis of the lower reactor internals, the turbulent pressure PSD spectra must be known in the regions where turbulent excitation is strongest. In the present case, the region of primary interest is the vessel downcomer. The mathematical expressions of such spectra typically have the form (Reference 5-1):

$$S_p(f) = ((\rho U^2)/2)^2 * (D/U) * \Phi(f^{**}) \qquad (5\text{-}1)$$

where ρ and U are fluid density and velocity, respectively, D is a characteristic length, $\Phi(f^*)$is a function of reduced frequency f**, which is defined as:

$$f^{**} = fD/U$$

and f is frequency in Hz. Test data for such spectra have been obtained for the 3XL internals configuration (Reference 5-2). The pressure PSDs measured in this test exhibit significant variations within the vessel downcomer and elsewhere, some of which can be attributed to variations in the fluid

velocity U and the rest to spatial variations in the function $\Phi(f^{**})$. For the 3XL configuration, the measured PSD data are available. A mathematical correlation using these data and the results of a CFD analysis using the CFX computer code (Reference 5-3) of the 3XL inlet nozzles, downcomer, and lower plenum was developed using the type of formulation described by Equation 5-1. The specific mathematical relationship used was:

$$S_p(f) = ((\rho U^2)/2)^2/(\xi)^*\Phi(f^*) \quad (5\text{-}2)$$

where reduced frequency f^* is now defined as $f^* = f/\xi$ and ξ is fluid vorticity. Fluid vorticity ξ replaces the quantity (U/D) in Equation 5-1 and in the definition of the reduced frequency. The idea here is to permit a greater generality than Equation 5-1 allows by defining the variations in PSD spectra in terms of parameters that are known to be related to turbulence generation, such as local velocity and local vorticity. The observed sensitivity of the measured PSD functions to local flow field variations (Reference 5-2) is more readily simulated by Equation 5-2 than by Equation 5-1.

A CFD analysis of the AP1000 downcomer and lower plenum was then performed, and downcomer PSD levels were calculated using CFD-predicted variations in velocity and vorticity as input to the PSD correlation developed above. The steps in this process are outlined below and basically involve using the CFD predicted values of U and ξ in an equation like 5-2 to best fit the existing 3XL data. The correlation thus derived is then used—together with CFD calculations—to predict PSD spectra in the AP1000 plant. The complete flow-induced vibration procedure—including the development of the PSD spectrum correlation—is outlined in Figure 5-1.

- A detailed CFD model of the flow field in the 3XL reactor vessel was generated using the CFX code (Reference 5-3). The model covers the region just upstream of the reactor vessel inlet nozzles to approximately the mid-elevation of the core. Details—such as neutron pads, surveillance capsule specimen holders, core barrel lower restraint keys/clevices, and downcomer flow blockage due to core barrel outlet nozzles—are included in the model.

- Excitation force power spectral densities were generated by using the 3XL CFD results and 3XL scale model test data to define constants in an empirical function for $\Phi(f^*)$. The empirical function defines the fluctuating pressure power spectral density at a given location as a function of frequency f, calculated local vorticities ξ, and calculated local fluid velocities U that results in the best fit with experimental fluctuating pressure spectral densities from the 3XL flow testing. The form of the fluctuating pressure power spectral density function, $S_p(f)$, is:

$$S_p(f) = [C_1][(\rho U^2)^2/\xi]/[1 + C_2(f^*)^n + C_3(f^*)^{n/2}] \quad (5\text{-}3)$$

  where ξ is fluid vorticity, $f^*=f/\xi$, f is frequency (Hz), U is fluid velocity, and the quantities C_1, C_2, C_3 and n are determined by a best fit with the measured pressure power spectral densities. A comparison of the PSD correlation with the measured data is presented in Figure 5-2 for three locations in the 3XL test: transducers 85, 88, and 91. These are all in the 3XL scale model downcomer at progressively decreasing elevations with transducer 85 being nearest the inlet nozzle where the vorticity is strongest.

- The pressure spectra were integrated with spatial correlation length functions from the literature (Reference 5-4) to obtain a group of forces to be applied to the reactor vessel and core barrel downcomer surfaces.

- Horizontal and vertical excitation force power spectral densities for regions other than the downcomer were developed from tests and analyses on similar components.

- A fluid-structure model of the hot functional test configuration of the Doel 4 (3XL) reactor was made. This model simulates the reactor vessel and its supports, the control rod drive mechanisms (CRDMs), integrated head package (IHP), upper and lower reactor internals, and fluid. The core barrel and baffle-former are modeled as a shell. The lower support plate is modeled as a plate with equivalent elastic properties. The reactor vessel is modeled as a concentric beam connected to the internals at appropriate locations. The upper internals guide tube and support columns, and the bottom-mounted instrumentation and secondary core support structures are also modeled as equivalent beams. The reactor vessel support and primary loop piping stiffness at the reactor vessel nozzles are also represented in the system analytical model. The lower internals portion of this system model is illustrated in Figure 5-4.

- The natural frequencies obtained from modal analysis of the 3XL fluid-structure model were compared to those obtained from preoperational testing. Good correspondence between calculated and measured frequencies is shown in Table 5-1.

- Digital time histories were generated from the excitation force PSDs discussed above and applied to the fluid-structure model.

- The responses of the 3XL lower internals were compared to those obtained from the Doel 3 plant measurement program results over several frequency bands. Where differences were found between calculated and test results, adjustment factors were applied. The adjustment factors modified the forcing functions to refine the agreement between the measured and calculated results for the 3XL configuration. The results obtained with the final forcing functions are compared to the corresponding measurement results in Table 5-2. The comparison shows that the calculated results are conservative relative to the measurements for all but the measurements made with the radially sensitive, mid-elevation, core barrel accelerometers. The latter can be attributed to pressure sensitivity of the accelerometers. However, the non-linear runs were performed with adjustments to the downcomer PSD levels to cover the less than unity core barrel/reactor vessel downcomer ratios.

- A CFD model of the AP1000 inlet nozzle, downcomer, lower plenum, and a portion of the core was developed and used to define the flow fields in these regions. This model included a portion of the core since the hot, full-power responses were to be calculated.

- The downcomer excitation forces for the AP1000 design were generated by applying the methodology used to calculate forces for the 3XL design. The AP1000 downcomer forces were estimated from the correlations of pressure PSDs described above, using values of flow field velocity and vorticity form the AP1000 CFD calculations and spatial correlation functions from the literature. In general, the AP1000 forces were found to be larger than those of the 3XL design

in the region of the nozzle/downcomer and were distributed differently due to the differences between the inlet nozzle configurations. The AP1000 forces are lower in the middle region of the downcomer where the 3XL plant has neutron pads. Overall, the total force or moment acting on the core barrel (as a beam) is approximately equivalent. Stresses for the core barrel are within limits as shown in section 6.3.

- The velocities and vorticity levels in the CFD results for the lower vessel head plenum of the AP1000 design were compared to corresponding results for the 3XL design to determine the appropriate relative level of the turbulence forcing functions on the structures below the lower core support plate. This comparison indicated similar values for the two designs although the differences in lower plenum hardware, inlet nozzle configuration, and radial key locations resulted in some distributional differences.

- The remaining forces for the AP1000 analysis were obtained by adjustment of the corresponding 3XL forces for area and velocity differences. The factors for these adjustments are shown in Table 5-3.

5.2.2 Reactor Coolant Pump Speed Related Excitations

5.2.2.1 Hot, Full Power

The ACSTIC computer code (References 5-5 and 5-6) was used to evaluate the pump-induced vibration condition for the AP1000 upper support plate, lower support plate, guide tubes, and support columns. The entire primary system could not be modeled due to storage limitations. Therefore, a one half symmetry RCS model was used (two half-loops). The model consisted of the steam generator, RCP, hot leg, cold leg, reactor vessel, and internals. The nodes in ACSTIC represent subvolumes of the RCS and are connected by flow paths in one-, two-, or three-dimensional arrays. In the present model, the piping, steam generators, pumps, hot leg, and cold leg were simulated one-dimensionally; the vessel downcomer and core shroud region two-dimensionally; and the lower plenum, core, and upper plenum, three-dimensionally. Figure 5-3 illustrates the distribution of nodes in the reactor vessel. The ability of ACSTIC to analyze multi-dimensional wave propagation is demonstrated in Reference 5-6.

Forcing functions at the RCP were based on scale model test data at the one-per-revolution, first vane-passing, and second vane-passing frequencies:

- One-per-revolution (29.2 Hz): [ ]^{b,c} psi
- First vane-passing (204.6 Hz): [ ]^{b,c} psi
- Second vane-passing (409.2 Hz): [ ]^{b,c} psi

These levels were inferred by scaling to full-size conditions from the laboratory tests conducted for scale model AP600 pumps. The AP1000 pump design has a somewhat larger volume than the AP600 pumps, which should diminish the magnitude of fluctuations reaching the reactor vessel; however, the pump geometry was conservatively based on the AP600 design. In addition, a factor of increase in pump forcing function magnitudes over the AP600 values was applied, based on the pump head increase from AP600 to AP1000. These assumptions ensure that the calculated results are conservative.

The ACSTIC results yield radial, axial, and azimuthal gradients for the various components under investigation. The pressure gradients extracted from the ACSTIC results were tabulated for the upper and lower support plates, guide tubes, and support columns areas. The tabulated results in Tables 5-4 to 5-7 conservatively represent the maximum pressure load amplitudes over a (+/-) 10-percent band of frequencies around each of the three pump frequencies to allow for uncertainties in fluid properties, modeling details, and other effects. The maximum pressure for the guide tubes and support columns represents the maximum radial and azimuthal loads in the upper plenum. The guide tube and support column loads are at three elevations, (top, middle, and bottom). These maximum gradients were then compared to the results of reference plants in WCAP-10239 (Reference 5-7).

The upper support plate, lower support plate, core barrel wall, core shroud wall, and core barrel beam pressure loadings were evaluated at all three frequency ranges (29.2 Hz , 204.6 Hz, and 409.2 Hz), and the guide tubes and support columns were evaluated at the 204.6 Hz and 409.2 Hz frequency range. Two types of ACSTIC computer runs were used to evaluate the pump induced vibration issue: 1) All RCP pumps in phase, and 2) two RCP pumps 180 degrees out of phase with the two in the opposite loop. For the pump in-phase case, some loads like the core barrel beam loadings vanish by definition and have no entries in the table. Results for the upper support plate, lower support plate, core barrel wall, core shroud wall, and core barrel beam pressure loadings are listed in Tables 5-4 to 5-6 for both cases and compared to similar data for DOEL 4. The guide tube and support column results in Table 5-7 are the maximum over both in-phase and out-of-phase conditions. The calculated AP1000 maximum pressure gradients listed in Table 5-7 are compared to the TVA plant (Reference 5-7), which has similar guide tubes and support columns with acceptable pump-induced vibration levels. Pressure gradients for Sizewell B, a four-loop standard plant (that is, not UHI) are also shown in Table 5-6.

ACSTIC analysis results of reference plants have been compared to test data with good correlation (Reference 5-7). It is, therefore, expected that the results of the AP1000 ACSTIC analysis predict the responses in the AP1000 plant with reasonable accuracy.

5.2.2.2 Reactor Coolant System Heatup

During reactor coolant system heatup and cooldown, the AP1000 RCP are operated using a variable speed controller to limit the pump power to no greater than the hot full power requirement.

A tentative pump startup sequence form cold conditions is given in Table 5-7.

During RCS pump startup, the coolant temperatures vary from 70°F to 557°F and the rotational speeds vary from 200 rpm to 1750 rpm. Since pump excitation frequency is proportional to rotational speed and the coolant sound speed increases with temperature, the chances of passing through an acoustic resonant condition are high. Fortunately, the pump forcing functions at lower rotational speeds are proportional to the square of the rotational frequency. Specifically, the pump excitation varies as:

$$\Delta p \sim \rho \cdot f^2$$

where f is pump rotational speed and ρ is fluid density. Therefore, if the excitation Δp(ref) and density ρ(ref) at a reference frequency f(ref) condition are known, the excitation at the desired condition can be obtained from:

$$\Delta p = \Delta p(ref)*(\rho/\rho(ref))*(f/f(ref))^2 \quad (5\text{-}4)$$

In the present case, the reference condition is the hot, full-power condition, for which the following pertain for the one-per-revolution excitation and first vane-passing excitation:

f = 1750 rpm
Δp = [ ]^{b,c} psi (one-per-revolution)
Δp = [ ]^{b,c} psi (first vane-passing)
Δp = [ ]^{b,c} psi (second vane-passing)

Using the above conditions and Equation 5-4 to define the excitation magnitude, ACSTIC runs were made covering the pump frequency ranges identified above and their 7-times and 14-times vane-passing multiples. Table 5-8 summarizes the peak pressure difference pulsation amplitudes at several frequencies at which acoustic resonant amplification appeared to be notable.

5.2.2.3 Evaluation of Reactor Coolant Pump Pulsations During Heatup

Evaluation of the RCP loads during heatup are not expected to cause unacceptably high stresses. These loads are considered in the design of the AP1000 reactor internals.

5.2.3 Turbulence Excitation of the System Fundamental Acoustic Mode

Figures 5-5 through 5-8 show the full temperature, three RCP responses at Doel 4. The responses at [ ]^{b,c} Hz are attributed to the core barrel beam mode. The responses at [ ]^{b,c} Hz are not attributed to a core barrel beam mode since, for example, the phase difference between the signals from radially sensitive accelerometers mounted 180° apart at a mid-elevation of the core barrel is 180° and the response is not large, if present at all, in the core barrel flange strain gages. The first acoustic mode (that is, a compressible fluid mode having one full wavelength around the system of the AP1000 system) is at [ ]^{b,c} Hz.

The 8.25 Hz responses in the 3XL measurements are attributed to turbulence excitation of this mode. It is noted that at least part of the signal at this frequency in the accelerometers can be attributed to pressure sensitivity of the accelerometers. Additionally, it is reported that no [ ]^{b,c} Hz signal content was found in the signals from accelerometers mounted on the exterior of the reactor vessel.

Pressure differences were applied to the 3XL system model to establish a forcing function for this excitation. Vertical excitations were applied to the reactor vessel, the upper and lower support structures, and the core barrel flange. Horizontal excitations were applied to the core barrel wall. The relative magnitudes of the pressure applied to each component were taken as the relative magnitudes calculated for the fundamental system acoustic mode of the AP1000 ACSTIC model. To estimate the forcing function for this response for the 3XL design, a representation of the 3XL excitation was developed as sine waves at [ ]^{b,c} and [ ]^{b,c} Hz and included in the excitation forces applied to the 3XL system

model. The absolute magnitude was established by adjusting the forces so that the strain measured on the inner wall of the upper support structure skirt during the 3XL lower internals plant measurement program (Reference 5-8) was approximated. The displacement implied by the magnitude of the strain signal was multiplied by a strain per deflection factor determined by finite element analysis. The accelerometers installed for the measurement program were not used as the fundamental basis for this excitation because of their pressure sensitivity.

No magnitude adjustment was applied to this excitation for the corresponding AP1000 excitation since the average downcomer turbulence level is calculated to be the same for both designs. The fundamental system mode natural frequency of the AP1000 model is calculated to be 9.66 Hz. In addition to the differential pressure loads applied to the 3XL components, a differential pressure was also applied to the core shroud for the AP1000 analysis.

5.2.4 Vortex Shedding Excitation Forces

In addition to broadband flow turbulence excitation, sinusoidal vortex forces were applied to the vortex suppression plate and secondary core support plate structures. This was done for conservatism. Vortex shedding from these components has not been observed in test data for these structures.

Since the vortex shedding frequency for the cross-flow velocities and column diameter in the lower head plenum is well above the lower plenum structure fundamental natural frequencies (lowest structural natural frequency is $f_n \approx$ [ ]^{b,c} Hz; estimated drag direction shedding frequency is [ ]^{b,c}), the velocity was selected to provide coincidence with the core barrel beam mode. Lift and drag coefficients were taken from the literature.

Table 5-1 Comparison of Calculated to Measured 3XL Lower Internals Natural Frequencies

Mode	Direction of Analytical Mode	Calculated Natural Frequency (Hz)	Measured Natural Frequency (Hz)
Coolant pressure	Horizontal	[	] b,c
Core barrel beam	Horizontal		
Core barrel shell, n = 2, m = 1	Horizontal		
Core barrel shell, n = 3, m = 1	Horizontal		
Lower internals	Vertical		
Upper internals	Vertical		
Reactor vessel	Horizontal		
Reactor vessel	Horizontal Vertical		
BMI upper tie plate translation	Horizontal		
BMI upper tie plate torsion	Horizontal		
BMI lower tie plate translation	Horizontal		
BMI lower tie plate torsion	Horizontal		
Lower guide tube	Horizontal	[	]

a. Estimated from AP1000 ACSTIC model.

BMI = bottom-mounted instrumentation

Table 5-2 Comparison of Calculated to Measured 3XL Responses

Excitation		Frequency Band (Hz)	Calculated RMS Level (mils)	Measured RMS Level (mils)	Ratio of Calculated to Test
Location	Direction				
Core barrel/reactor vessel downcomer	Horizontal[a]	6 to 15	[	]b,c	0.80
	Horizontal[a]	15 to 50	[	]	0.74
Upper tie plate	Horizontal[b]	50 to 120	[	]	1.81
Lower tie plate	Horizontal[b]	15 to 50	[	]	0.91
			[	]	
Reactor vessel	Vertical	6 to 15	[	]	
Lower core support plate	Vertical	5 to 15	[	]	0.44
Lower core support plate	Vertical	15 to 50	[	]	1.84
Upper support plate	Vertical	5 to 15	[	]	1.08
Upper support plate	Vertical	15 to 50	[	]	0.88
Upper support plate	Vertical	50 to 120	[	]	N/A

a. Average of three radial locations
b. Vector displacement
c. Includes some content due to rocking
d. The accelerations are considered to be influenced by accelerometer pressure sensitivity. The vertical vibration content in the core barrel strain gages is difficult to ascertain because of masking by other contributors. There is believed to be a large contribution at [ ]b,c Hz related to pressure sensitivity of the accelerometer.

NA = not applicable

Table 5-3 Summary of 3XL to AP1000 Flow Turbulence Excitation Conversion Factors

Force Location	Force Direction	Force Elevation	Bases for Conversion Factor	Force PSD Conversion Factor	
RV lower head	Horizontal	~~15 in below LCSP (CG of lower plenum)	Vert. Ht. X RV dia. at bottom of LCSP, downcomer exit velocity raised to a power of 4		b,c
RV lower head	Vertical	—	(Downcomer exit velocity)[c] x (RV ID)[b]		
Upper tie plate	—	—	—		
Lower tie plate	Horizontal	Mid-elevation of lower tie plate	(No. of cols)(D)[b](L/D)(downcomer exit velocity raised to a power of 4)		
SCSP	Horizontal	Mid-elevation of SCSP	Same fraction as used on Tsuruga		
Upper tie plate	Torsion	—	—		
Lower tie plate	Torsion	—	Square of outer column radius x force PSD		
Guide tubes	Horizontal	Mid-plenum elevation[a]	No of guide tubes x maximum mean load[b]		
Guide tubes	Torsion	Mid-plenum elevation[a]	Same radius of gyration as for 3XL		
Upper support columns	Horizontal	Mid-plenum elevation[a]	No of support cols x maximum mean load		
Upper support columns	Torsion	Mid-plenum elevation[a]	Same radius of gyration as for 3XL		
LCSP	Vertical	—	Inlet flow hole vel. raised to a power of four		
Upper support structure	Vertical	—	(Out. noz. V x noz. ID)[c] (no. of noz.)(core barrel ID)[b]		
Upper core barrel wall	Horizontal	(a)	(Out. noz. V x noz. ID)[c] (no. of noz.)(core barrel ID)(upper plenum length)		
Fuel assembly force PSDs are scaled from Tsuruga 3/4 PSDs (since the hot functional test configuration was modeled for the 3XL analysis).					
Fuel assemblies	Horizontal	71.6 and 156.2 in. Above top of LCP	No. and length of assemblies, no. of grids, flow velocity		
Fuel assemblies	Vertical	—	No. of assemblies, no of grids, flow velocity		
Core shroud[c]	Horizontal	(To be established)	Core width (no. of assemblies), length of assemblies, number of grids, flow velocity		

a. Same elevation as used for the 3XL analysis
b. Very conservative, based on the locations of the added components
c. These forces are negligible relative to the downcomer force –induced responses of the core shroud (and core barrel)

Definitions:
FLTP = lower tie plate
LCSP = Lower core support plate
RV = Reactor vessel
SCSP = Secondary core support plate

Table 5-4 ACSTIC Results for Upper and Lower Support Plates, Over 26.5 to 32.5 Hz Range, Hot, Full-Power Condition

Component	Frequency (Hz)	Location	Calculated Maximum Difference	
			AP-1000	3XL (Doel 4)
Vertical				
Upper support plate (193-210)	29 Hz range pumps in phase	Average[(b)] over surface	[	] b,c
	29 Hz range pumps out of phase	Average[(b)] over surface		
Lower support plate	29 Hz range pumps in phase	Average[(b)] over surface		
	29 Hz range pumps out of phase	Average[(b)] over surface		
Core barrel flange	29 Hz range pumps in phase	Average[(b)] over surface		
	29 Hz range pumps out of phase	Average[(b)] over surface		
Lower support plate rim to core shroud cavity	29 Hz range pumps in phase	Average[(b)] over surface		
	29 Hz range pumps out of phase	Average[(b)] over surface	]	]
Horizontal				
			Beam	**Wall**
Core barrel[(a)] wall	29 Hz range pumps in phase	Upper end Mid-elevation Lower end	[	] b,c
	29 Hz range pumps out of phase	Upper end Mid-elevation Lower end		
Core shroud	29 Hz range pumps in phase	Upper end Mid-elevation Lower end		
	29 Hz range pumps out of phase	Upper end Mid-elevation Lower end	]	]

a. Maximum around circumference
b. For small values, the maximum is listed.

Table 5-5 ACSTIC Results for Upper and Lower Support Plates, Over 176 to 212 Hz Range, Hot, Full-Power Condition

Component	Frequency (Hz)	Location	Calculated Maximum Difference	
			AP-1000	3XL (Doel 4)
Vertical				
Upper support plate	204 Hz range pumps in phase	Average[(b)] over surface	[	] b,c
	204 Hz range pumps out of phase	Average[(b)] over surface		
Lower support plate	204 Hz range pumps in phase	Average[(b)] over surface		
	204 Hz range pumps out of phase	Average[(b)] over surface		
Core barrel flange (Also called "DC to upper head")	204 Hz range pumps in phase	Average[(b)] over surface		
	204 Hz range pumps out of phase	Average[(b)] over surface		
Lower support plate rim to core shroud cavity	204 Hz range pumps in phase	Average[(b)] over surface		
	204 Hz range pumps out of phase	Average[(b)] over surface	]	]
Horizontal				
			Beam	**Wall**
Core barrel[(a)] wall	204 Hz range pumps in phase	Upper end Mid-elevation Lower end	[	] b,c
	204 Hz range pumps out of phase	Upper end Mid-elevation Lower end		
Core shroud[(a)] wall	204 Hz range pumps in phase	Upper end Mid-elevation Lower end		
	204 Hz range pumps out of phase	Upper end Mid-elevation Lower end	]	]

a.. Minimum around circumference
b. For small values, the maximum is listed.

Table 5-6 ACSTIC Results for Upper and Lower Support Plates, Over 372 to 454 Hz Range, Hot, Full-Power Condition

Component	Frequency (Hz)	Location	Calculated Maximum Difference	
			AP-1000	3XL (Doel 4)
Vertical				
Upper support plate	407.8 Hz range pumps in phase	Average[b] over surface	[	] b,c
	407.8 Hz range pumps out of phase	Average[b] over surface		
Lower support plate	407.8 Hz range pumps in phase	Average[b] over surface		
	407.8 Hz range pumps out of phase	Average[b] over surface		
Core barrel flange (also called 'DC to upper head')	407.8 Hz range pumps in phase	Average[b] over surface		
	407.8 Hz range pumps out of phase	Average[b] over surface		
Lower support plate rim to core shroud cavity	407.8 Hz range pumps in phase	Average[b] over surface		
	407.8 Hz range pumps out of phase	Average[b] over surface	]	]
Horizontal				
			Beam	**Wall**
Core barrel[a]	407.8 Hz range pumps in phase	Upper end Mid-elevation Lower end	[	] b,c
	407.8 Hz range pumps out of phase	Upper end Mid-elevation Lower end		
Core shroud[a]	407.8 Hz range pumps in phase	Upper end Mid-elevation Lower end		
	407.8 Hz range pumps out of phase	Upper end Mid-elevation Lower end	]	]

a. Maximum around circumference
b. For small values, the maximum is listed.

Table 5-6 (cont.) ACSTIC Results for Upper and Lower Support Plates, Over 372 to 454 Hz Range, Hot, Full-Power Condition

Component	Frequency (Hz)	Location	Calculated Maximum Gradient		
			AP1000	Sequoyah 1	Sizewell B
Guide tubes	204	Top			[[ ]]b,c
		Middle			
		Bottom			
	409	Top			
		Middle			
		Bottom			
Support columns	204	Top			
		Middle			
		Bottom			
	409	Top			
		Middle			
		Bottom			

Table 5-7 Estimated Operating Conditions for AP1000 Plant/Reactor Coolant Pump Startup from Cold Conditions Using Variable Frequency Drives – All Four Pumps Running[a]

Time (min)	RCS Temp (°F)	Speed (rpm)	Head (ft)	Flow/Pump (gpm)	Total Flow (gpm)
0	70	200	5	9,000	36,000
3	70	1600	322	74,000	288,000
360	231	1600	322	74,000	288,000
361	231	1680	335	75,500	302,000
840	450	1680	335	75,500	302,000
841	450[b]	1750	365	78,750	315,000
1080	557	1750	365	78,750	315,000

a. The pumps are started one at a time, maintaining the low speed as given at time zero until all four pumps are running. From then on, the speed of all four pumps is increased together.

b. At RCS temperatures >450°F, the variable frequency drives are switched out and the pumps are operated at constant speed.

Table 5-8 Peak Pressure Difference Pulsation Amplitudes During Heatup

Component	[ ]b,c Hz[a]	60.8 Hz	139 Hz	185-188 Hz
Upper support plate				]b,c
Lower support plate				
Lower core barrel wall				
Downcomer to upper head				
Upper core barrel wall				
Upper core shroud				
Lower core shroud				
Lower plenum to upper head				
Guide tube support columns				

a. The [ ]b,c Hz in the above table is essentially the once-around-the-loop mode, which, at full-power conditions, has a frequency on the order of [ ]b,c Hz. The increase to [ ]b,c Hz is due to the higher fluid sound speed at 70°F.

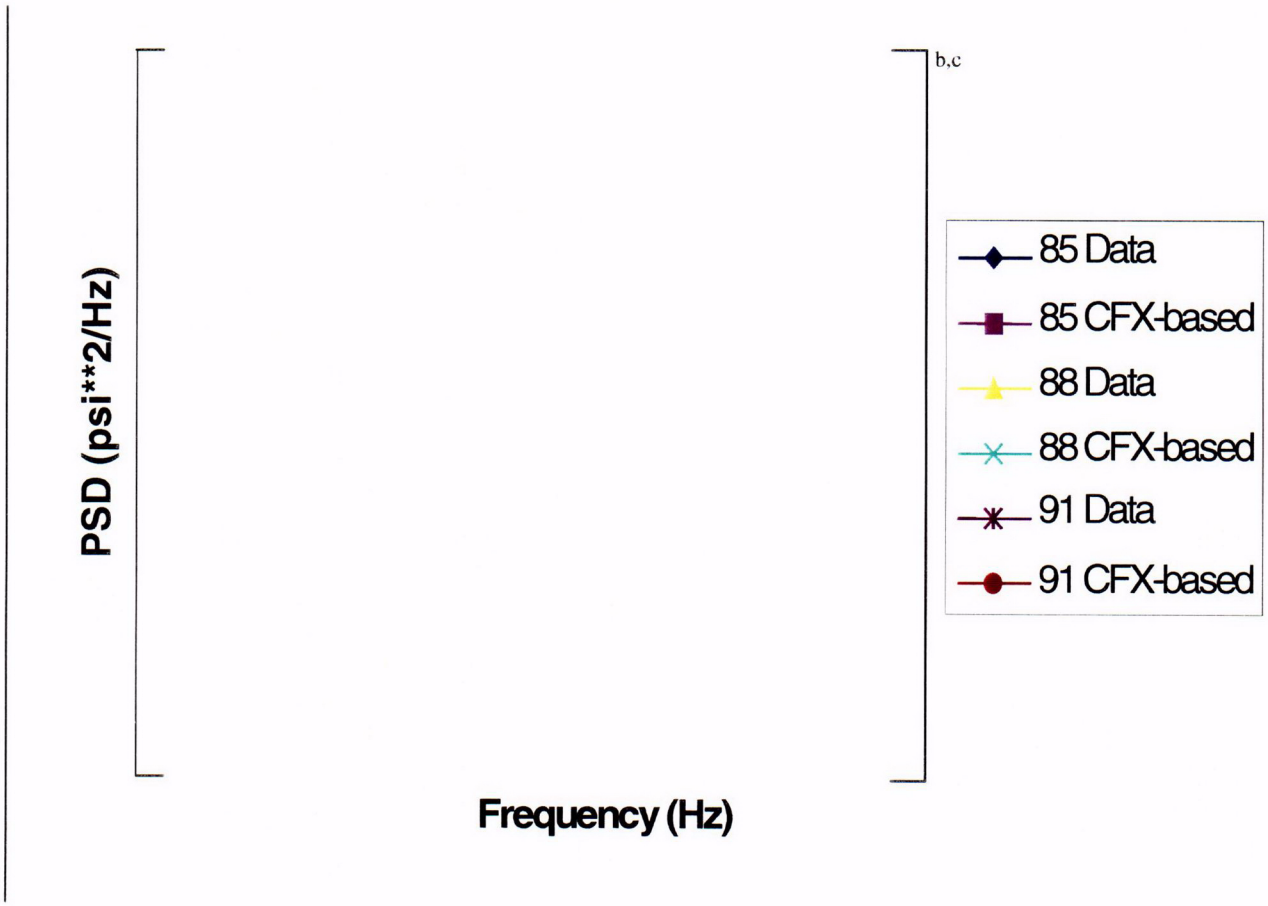

Figure 5-2 3XL PSD: Data Bases 85, 88, and 91: PSD Data Versus Correlation in Vessel Downcomer

C01

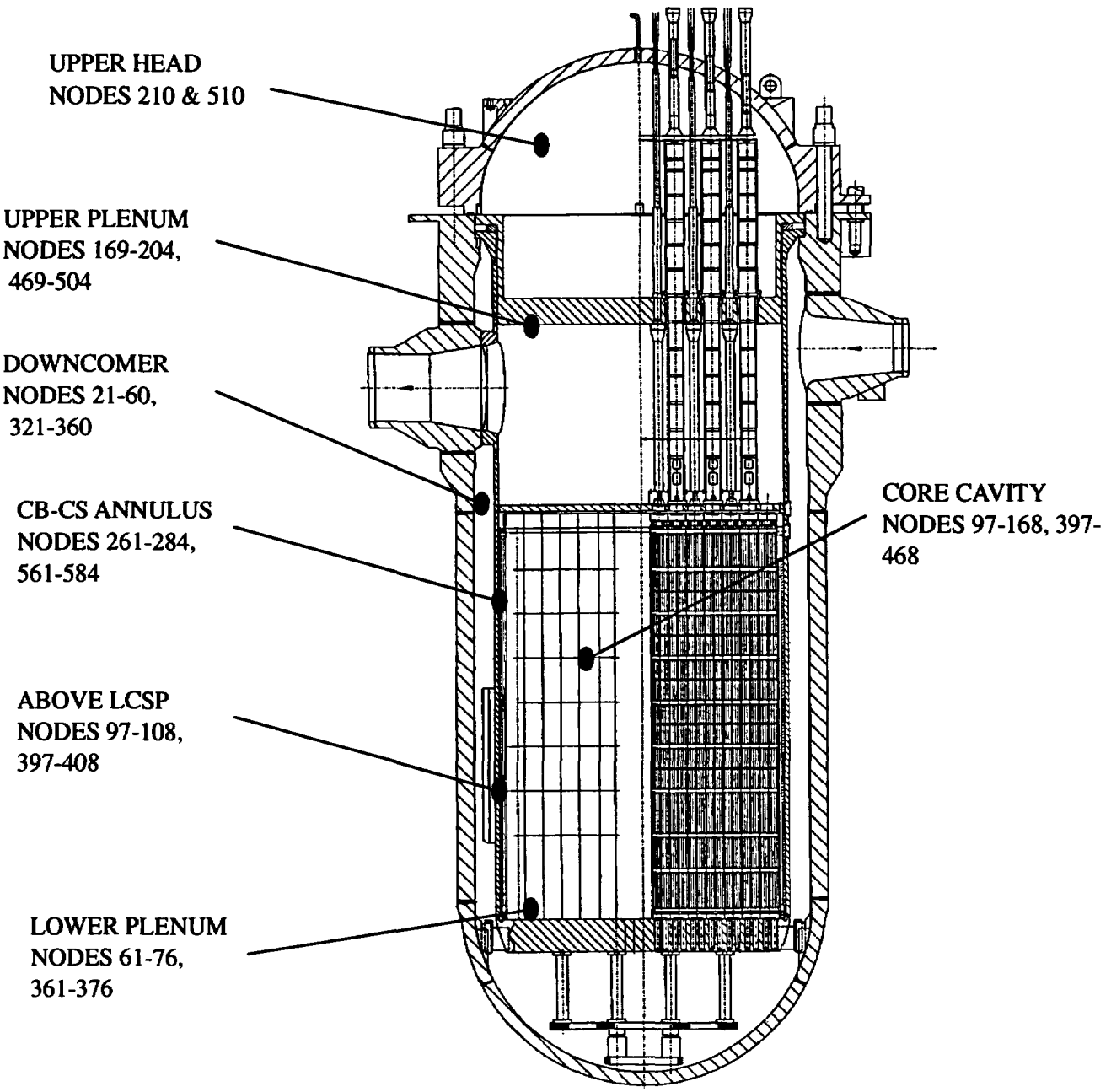

Figure 5-3 Distribution of ACSTIC Nodes in AP1000 Reactor Vessel

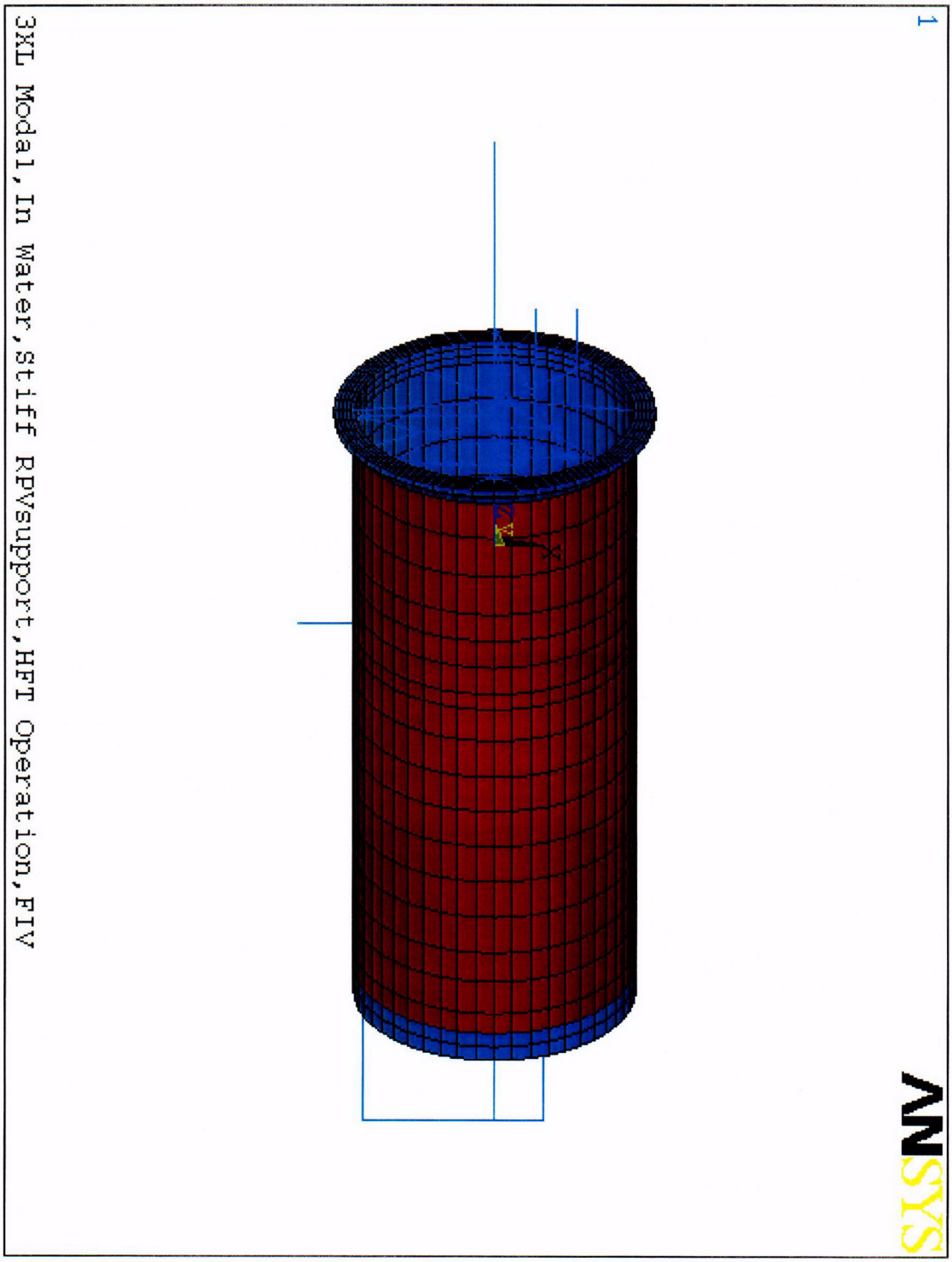

Figure 5-4 3XL System Model

C02

Figure 5-5 Axially Sensitive Strain Gage on Outer Wall of Core Barrel, Below Flange, 0°

Figure 5-6 Vertically Sensitive Accelerometer on Lower Surface of Lower Core Support Plate, Near Center


b,c

Figure 5-7a Radially Sensitive Accelerometer at Approximately Mid-Elevation of Core Barrel, 0°


b,c

Figure 5-7b Radially Sensitive Accelerometer at Approximately Mid-Elevation of Core Barrel, 305°

Figure 5-8a Axially Sensitive Strain Gage on Inner Wall of Upper Support Plate Skirt, 180°

Figure 5-8b Vertically Sensitive Accelerometer Upper Surface of Upper Support Plate, Near Centerline

6 EVALUATION OF AP1000 VIBRATION RESPONSES

6.1 AP1000 REACTOR SYSTEM MODEL

A finite element model of the AP1000 system similar to that made for the 3XL design was developed (Figures 6-1 through 6-7). In the AP1000 model, the core shroud (Figure 6-7) was modeled as a shell. The structures below the lower core support plate were modeled as a beam similar to the modeling of the lower tie plate structure of the 3XL design. Models were made for the hot functional test condition and for the hot, full-power condition.

6.1.1 Evaluations Performed

The force time histories, which were developed as described in section 5, were applied to several model key/clevis gap configurations for the hot, full-power condition. Results from the AP1000 displacement calculations are reviewed to determine the following:

- RMS displacements (see section 6.2) are reviewed at key locations on the core barrel, reactor vessel, and internals. These provide a measure of relative difference of the AP1000 response. These results also are used in defining expected hot functional test transducer responses summarized in section 7. The displacements are also used to verify that the peak-to-peak vibration amplitudes are smaller than the clearances provided in the AP1000 reactor vessel and internal design.

- Fatigue stresses (see section 6.3) are evaluated for the lower and upper internals and core support structures.

- Interface loads (see section 6.4) are reviewed to do the following:

  - Determine the cases that produce the highest forces and determine what peak forces should be compared to design values for the following key interfaces:

    - Core barrel/upper core plate interface
    - Core barrel/lower core support plate interface
    - Core shroud/core barrel upper interface

  - Determine the peak-to-peak horizontal shear force and moment that the core barrel clamping force must resist

6.2 RMS DISPLACEMENTS

The response time history RMS displacements due to broadband flow turbulence and the turbulence-excited acoustic mode that were calculated using the AP1000 System Model are listed in Table 6-1. The corresponding 3XL results at key locations are also listed in the table.

These results indicate that:

- The core barrel displacements of the AP1000 design are acceptable. The ratio of the AP1000 core barrel displacements to the 3XL core barrel displacements varies with location on the core barrel. The maximum ratio is approximately 150 percent at the middle elevation and approximately 120 percent at the lower support plate elevation.

- The calculated 3XL displacements using the same modeling techniques as applied for the AP1000 were greater than those observed in the 3XL test results. Therefore, the calculated AP1000 displacements are judged to be conservative.

6.3 EVALUATION OF AP1000 VIBRATION-INDUCED FATIGUE STRESSES

6.3.1 Lower Internals

A finite element model of the AP1000 design was developed (Figure 6-8) and analyzed for forces described in section 5.

For the evaluation of lower internals fatigue stresses, a zero-to-peak to RMS ratio of [ ]^{b,c} is included for turbulence excitation. The RCP-related responses are calculated for the worst pump phasing. The stress levels from the two sources are added algebraically.

The time histories of the fluid-structural model were examined for the times and gap patterns that produce the highest lower internals stresses. Having chosen the highest stress-producing gap configuration and time, submodels were made of the areas indicating the highest stresses. This was done to determine the levels to be used in determining the fatigue factor of safety for the lower internals.

The AP1000 lower internals core barrel assembly has the same wall thickness and inside diameter as the 3XL plants. Both the AP1000 and the 3XL plants use a single integrated lower core support plate attached to the core barrel with a circumferential full penetration girth weld.

6.3.1.1 Core Barrel

The peak stress intensity in the core barrel/lower core support plate is at the barrel wall to flange intersection (Figure 6-2) and is [ ]^{b,c} psi. The peak stress in the core barrel/lower core support plate is less than the allowable alternating stress of 13,000 psi at 10^{11} cycles from the American Society Mechanical Engineers (ASME) Code, Appendix I, Figure I-9.2.2 (Curve C). The fatigue stress margin – which is the ratio between the allowable alternating stress and the calculated peak stress minus one – is [ ]^{b,c}.

6.3.1.2 Core Shroud

The maximum stress intensity in the core shroud (Figure 6-7) is [ ]^{b,c} psi and is less than the allowable stress of 13,000 psi at 10^{11} cycles referenced above. The fatigue stress margin is at least [ ]^{b,c}.

6.3.2 Vortex Suppression Plate and Secondary Core Support Structures

The vortex suppression plate (VSP) has a larger surface area and more closely approaches the lower reactor vessel head than the lower tie plate system of the 3XL design. Estimates of turbulence excitation forces and forces due to the postulated periodic shedding of vortices were calculated in a conservative manner. The resulting forces were included with the broadband turbulence excitations in the excitations applied to the reactor vessel system model.

To calculate the modal properties of the structures below the lower core support plate, a finite element model was made of the structures (Figure 6-8). This model was also used in the determination of the high cycle fatigue stresses of these structures. The translational and moment forces due to broadband turbulence and the forces induced by vortex shedding were applied directly to the element of the finite element model. In addition, a base motion obtained from the lower core support responses of the system model due to flow turbulence, RCP speed-related, and acoustic modes was applied to the model.

The resulting margins (allowable stress/calculated value -1) are listed in Table 6-2. The minimum margin is 1.9.

6.3.3 Upper Internals

6.3.3.1 Upper Support Skirt and Flange

This section evaluates the high cycle fatigue margin of the upper support structure, as well as the upper support plate at the perforated region and skirt transition region.

RCP speed-related pulsations, local flow turbulence, and turbulence excitation of the system acoustic mode and upper core plate vibration are the excitations acting on the upper support plate. The AP1000 upper support plate zero-to-peak vibration is:

[ ] b,c

[ ]b,c

This deflection, multiplied by the maximum stress to USP center deflection ratio gives the maximum stress, $\sigma_{USP, max}$, of the AP1000 upper support skirt and flange:

$\sigma_{USP,max}$ = [ ]^{b,c};
$\sigma_{USP,max}$ = [ ]^{b,c} psi

The calculated stress for the upper support plate, compared to the allowable alternating stress of 13,000 psi at 10^{11} cycles from the ASME Code Figure I-9.2.2 Curve C, gives a margin of safety of [ ]^{b,c}.

6.3.3.2 Upper Support Plate and Skirt Transition

Using the calculated deflection above, the perforated region and skirt transition margins are calculated.

For the perforated region, the calculated maximum stress is [ ]^{b,c} psi. This alternating peak stress is well below the allowable alternating stress of 13,000 psi at 10^{11} cycles from the ASME Code Figure I-9.2.2 Curve C.

At the transition locations of the skirt, the calculated maximum stress is [ ]^{b,c} psi. This alternating peak stress is also well below the ASME allowable alternating stress.

6.3.3.3 Guide Tubes and Support Columns

Methodology

The guide tubes in the AP1000 upper internals are similar to the 17x17 AS guide tubes, and the support columns are identical to those in standard plants such as Doel 3 so that flow-induced vibration and load correlations can be confidently applied to the AP1000 components.

To calculate the high cycle fatigue margins of the guide tubes and support columns, the following methodology was used:

- A CFD model of the 3XL upper internals flow paths during the hot function test was made on the CFX computer code (Reference 5-3). The extent of this model was from the upper end of the core cavity to the outward end of the reactor vessel outlet nozzles.

- The mean flow loads on the most highly loaded guide tubes and support columns in the 3XL design were calculated and compared to measured values. No adjustments were necessary.

  The mean flow loads on the most highly loaded AP1000 components were calculated on a CFD model that corresponded closely to that of the 3XL design. The AP1000 upper internals have more guide tubes and support columns than the Doel 3 plant as discussed in section 3.1. The CFX model includes the AP1000 number of guide tubes and support columns as well as the AP1000 outlet nozzle geometry.

- The moments and forces at key locations of the AP1000 components were determined by scaling the measured 3XL responses to the AP1000 flow condition.

- The mean loads, and the moments and forces for quasi-static, first mode, and second mode frequency bands were determined from the RMS signal levels of the strain gages mounted on the guide tubes and support columns in the 3XL upper internals prototype measurement program.

- For the quasi-static vibration and the modal responses, the moments inferred from the strain gages were scaled by the ratio of the square root of the product of the mean force squared times the eigenvector squared summed over the length of the component.

- The moments and shear forces due to the flow loads for each frequency band discussed above were added as the square root of the sum of the squares at key locations.

- The RCP-induced excitations were added algebraically at each location.

- The moments due to core plate motion were added as the square root of the sum of the squares to the forces from directly impinging flows.

- The moments and shear forces at each cross section were compared to acceptable values to determine the component factor of safety for high cycle fatigue. The acceptable values were obtained from a finite element stress model and ASME code allowable stresses.

Measured and calculated steady flow loads for the three-loop standard configuration (Doel 3) are compared in Table 6-3. The measured loads were obtained from Reference 6-1. As shown in the table, steady flow loads predicted from 3XL 1/7 scale model data were somewhat greater than those measured in Doel 3, demonstrating the conservatism of the model results. Loads resulting from the CFD analyses were higher or about the same as the measured levels for five of the six components. The guide tube flow loads from the CFD calculation are 1.20 to 1.62 times the measured loads. The calculated upper support column mean flow loads are 0.83 to 1.09 times the measured loads. For one of the upper support column

locations (M-3), the calculated load was 86 percent of the load inferred from the scale model measurement and 83 percent of the load inferred from plant test measurements. These variations in load are small compared to the support column margins to allowable stresses (minimum margin of 2.1).

The calculated steady flow forces calculated for the most highly loaded components in the AP1000 plant are compared to the corresponding Doel 3 forces in Table 6-4. The mean flow forces on the AP1000 components are higher than those on the 3XL components; however, as shown in Figures 6-9 and 6-10, the additional loads are primarily away from the mid-elevation of the components. This reduces their effects on component fatigue stress relative to the effects if the additional loads were uniformly distributed.

Guide Tube High Cycle Fatigue Analysis

As discussed previously, the moments from each of the excitations are combined at each of the locations of interest along the guide tube. For the bottom flange weld, the shear forces become relatively important as compared to the bending moments. Therefore, the shear forces are also derived for the bottom flange weld. For the support pins, the reaction forces are combined.

These summed moments and forces are then used to scale high cycle fatigue alternating stresses associated with moments and forces used in previous analyses for the 17x17 AS guide tube with the design support pins. The moments and forces are combined for each of the specific stress locations by the following formula:

$$F_T = [F_1^2 + F_2^2 + F_3^2]^{1/2} + F_4$$

$$M_T = [M_1^2 + M_2^2 + M_3^2]^{1/2} + M_4$$

where:

M_T, F_T = Total moment, force
M_1, F_1 = Low frequency moment, force
M_2, F_2 = First and second modal moment, force combined by square root sum of the squares (SRSS)
M_3, F_3 = Core plate motion moment, force
M_4, F_4 = 204 Hz RCP-induced response

The first three excitations are random in nature; therefore, they are added as the square root of the sum of the squares. Since the fourth excitation is high frequency and is more deterministic, it is added algebraically. Each of the RMS levels of the moments and forces above, except for the RCP-induced are converted to zero to peak values by multiplying the RMS values by 4.5. For the deterministic RCP-induced moments and forces, the ACSTIC run already includes the maximum zero to peak pressure gradients due to the worst phasing between pumps. Therefore no RMS multiplier is needed. To compare to other plant data not including the RCP second blade passing frequency, the ratio of zero to peak to mean intermediate flange moment is [ ]^{b,c}. This is reasonable compared to measured best-estimate plant data for 17x17AS lower guide tubes, which range from [ ]^{b,c}.

Guide tube natural frequencies occur at frequencies close to the first and second harmonics of the RCP blade passing frequencies in the AP1000 design. Although greater separation of these frequencies is desired, it is noted that: Analysis of guide tubes for other plants made for similar differences between pump blade passing frequencies and guide tube natural frequency have shown that the resulting guide tube stresses are well within allowable values.

Detailed stress analysis for the 17x17AS guide tube was performed in Reference 6-2. In this document, the intermediate flange-to-enclosure weld throat primary and secondary tensile and shear stresses are related to a bending moment. These stresses are scaled to the corresponding AP1000 bending moment. For welds, per the ASME Code, Subsection NG, a stress concentration factor of 4 is used. The total stress intensity, corrected for the elastic modulus used for the ASME code design fatigue curve results in a high cycle fatigue alternating stress intensity value. The allowable value is taken from the ASME code, Figure I-9.2.2 for the endurance limit of welds and adjacent base metal at 10^{11} cycles. The result indicates a margin (allowable/actual –1) of 4.6.

A similar procedure is used to determine the margin at the continuous section card/enclosure pin and pin weld and the bottom flange/enclosure weld.

Using the guide tube model, and applied loads for the AP1000 reactor, the force on support pin is determined and the stress at the highest stress location is determined. Based on a finite element model of the pin, the pin loads are related to stress.

The resulting margins, summarized in Table 6-5 indicate a minimum guide tube fatigue margin high cycle fatigue of 0.6 to code allowable stresses. The margin of safety for all guide tube fatigue assessments is acceptable.

Upper Support Column High Cycle Fatigue Analysis

To determine the high cycle fatigue margins for the upper support columns, the moments due the quasi-static, modal core plate and RCP responses were combined at locations of interest. The margin to ASME code allowable values was then determined at each location. The results, listed in Table 6-6 indicate a minimum margin of 2.1, which is acceptable.

6.3.3.4 Fluidelastic Stability Evaluation for Guide Tubes and Support Columns

From Appendix N of the ASME Boiler and Pressure Vessel Code (1998 Edition, 2000 Addenda), the minimum fluidelastic constant for any array type is $\beta = 2.4$. For a square array (Reference 6-3):

$$\beta = 0.37 + 1.76\frac{T}{D}$$

Between a guide tube and support column,

$$T = \text{pitch} = 8.466\ \text{in.}$$

$$D = \text{width(avg)} = \frac{7.46\ \text{in.} + 3.50\ \text{in.}}{2} = 5.48\ \text{in.}$$

using the Type 1 support column. Therefore,

$$\beta = 0.37 + 1.76\left[\frac{8.466\ \text{in.}}{5.48\ \text{in.}}\right] = 3.0$$

$\beta > \beta_{min}$, so 2.4 will be used to find U_c.

$$U_c = (f_n)(D)(\beta)\left[\frac{(m_0)(\delta_n)}{(\rho\rho)(D)^2}\right]^{1/2}$$

where:

f_n = 1st mode natural frequency (62 Hz)
D = outside diameter (7.46 in)
β = fluidelastic constant (2.4)
m_0 = mass per unit length (4.442 lbm/in)
δ_n = logarithmic decrement of damping (0.176)
ρ = fluid density (0.0245 lbm/in^3)

Substituting:

$$U_c = (62)(7.46)(2.4)\left[\frac{(4.442)(0.176)}{(0.0245)(7.46)^2}\right]^{1/2} = 841\,\text{in/s} = 70\,\text{ft/s}.$$

Similarly, the support column has the following values for the variables:

f_n = 1st mode natural frequency (102 Hz)
D = outside diameter (3.5 in)
β = fluidelastic constant (2.4)
m_0 = mass per unit length (4.442 lbm/in)
δ_n = logarithmic decrement of damping (0.088)
ρ = fluid density (0.0245 lbm/in^3).

Substituting these values into the velocity equation:

$$U_c = (102)(3.5)(2.4)\left[\frac{(4.442)(0.088)}{(0.0245)(3.5)^2}\right]^{1/2} = 977\,\text{in/s} = 81.4\,\text{ft/s}$$

By comparison, the maximum value of the velocity calculated by CFD analysis using the CFX computer code (Reference 5-3) in the region of the guide tube and support column is 40.6 ft/s. Because this velocity is much lower than 70 ft/s and 81.4 ft/s, there is a margin of 1.7 for the guide tube and 2.0 for the support column, respectively.

6.4 INTERFACE LOADS

6.4.1 Methodology

A calculation of the vibratory force at interface of the AP1000 reactor internals has been carried out to estimate the flow and RCP induced forces for the following interfaces:

- Core barrel flange clamping
- Bolts at the core shroud to lower core support plate intersection
- Core barrel to reactor vessel keys and clevises
- Upper core plate to core barrel keys and clevises
- Core shroud to core barrel keys and clevises

6.4.2 Core Shroud to Lower Core Support Plate Bolts

6.4.2.1 Vibratory Loads

Sixteen bolts attach the lower end of the core shroud to the lower core support plate. In the system model 16 connections are represented. These are the only connections between the two structures in the analysis model. The hot, full power RMS forces due to flow forces calculated for these interface structures are listed in Table 6-7.

Taking that all of the forces are correlated, the needed preload to resist relative horizontal motion at hot, full power is:

$$\mu[F_P-(4.5)(.85)F_v] = [4.5][F_S]$$
$$F_P= [4.5][F_S/\mu +(.85)F_v]$$

In this, the 0.85 factor is taken as the fraction of the load that goes into the core shroud flange part of the joint. The sums of the individual forces were obtained by summing the time histories and finding the RMS value. If the sums are used,

F_P = [ ]b,c

or 23,670 lbs per bolt (or per 1/16 circumference) net preload.

This method does not assure that local relative motion will not occur; that is, under one or a few bolts. If the forces from the four most highly loaded adjacent bolts are added as the SRSS, the resulting needed preload per bolt at hot, full power (or per 1/16 of the circumference) would be:

[ ]b,c

An estimate of the effects of 9.6 Hz and RCP rotating speed excitation increases this force to about [ ]^{b,c} lbs.

The loads entering into the vertical force between the lower flange of the core shroud and the upper surface of the lower core support plate are listed and summed in Table 6-8. The net preload between the core shroud and the lower core support plate during normal operation is [ ]^{b,c} lbs. The margin to resist relative motion is [ ]^{b,c}, which is judged to be acceptable.

6.4.3 Core Barrel Flange Clamping

6.4.3.1 Vibratory Loads

The vector vibratory shear, S_V, and moments, M_V, at the core barrel flange resulting from flow turbulence excitation (vertical and horizontal) acoustic turbulence loads and RCP pressure pulsations are combined. The results are summarized in Table 6-9. Note that, for the linear cases, the RMS levels are multiplied by 4.5.

6.4.3.2 Needed Clamping Force

The needed clamping forces on the core barrel and upper support plate flanges to resist the vibratory shear force are:

$$\mu[P_{LI} + P_{UI}] = [4.5][S_{VLI} + S_{VUI}] \text{ or } [P_{LI} + P_{UI}]/[4.5][S_{VLI} + S_{VUI}] = 5.0 \quad (6.4\text{-}1)$$

where $P_{LI} + P_{UI}$ are the normal force acting between the lower surface of the core barrel flange and the reactor vessel ledge, and the normal force acting between the upper surface of the upper support flange and the reactor vessel head flange. A second evaluation is:

$$[P_{LI} + P_{HDS}]/[4.5][S_{VLI}] \geq 5.0 \quad (6.4\text{-}2)$$

where P_{HDS} is the vertical force of the core barrel hold down spring.

The clamping force needed can be estimated by two methods. The first is to take the clamping moment as the spring force times the radius of the load line. The radius is 67.99 in. to the contact point of the core barrel flange (and 71.06 in. to the contact point on the upper support structure flange).

With this method,

$$(P_{HDS})(R_c) = (4.5)(M_V) \quad (6.4\text{-}3)$$

Here M_V is the higher of the moments in the X- and Y-directions.

The preferred method, especially for evaluation of the normal operating condition is to take the force per inch that the vibratory forces produce around the circumference of the flange varies linearly like a stress cross section. Then the pressure per inch of circumference is related to the vibratory moment by:

$$P = 4.5M_V/\pi R^2 \text{ lb}_f\text{/in.} \quad (6.4\text{-}4)$$

For a spring of P_{HDS} lbs, $P = P_{HDS}/(2\pi R)$, and from Equation 6.4-3:

$$P[2\pi R][R] = (4.5)(M_V);\ P = 4.5M_V/2\pi R^2 \qquad (6.4\text{-}5)$$

Thus the first method (Equation 6.4-4) requires twice the load as the second method, (Equation 6.4-5) and will be used here. Thus the minimum load is defined by Equation 6.4-4.

Based upon the equations above and taking no credit for the hold down spring in available shear resistance, a spring load of approximately [ ]^{b,c} lbs at hot, full power will prevent uplift or sliding of the internal flanges relative to the vessel.

6.4.4 Key/Clevis Interfaces

The key/clevis interface loads calculated for the AP1000 design at hot, full-power are listed in Table 6-10. The maximum loads are in bold face type.

Based upon a fatigue limit of 13,000 psi, the allowable key interface force at the core barrel/reactor vessel location is [ ]^{b,c} lbs. The fatigue stress margin for the core barrel/reactor vessel location is [ ]^{b,c}.

Both the upper core plate/core barrel and upper core plate/core shroud interfaces have fatigue limits of more than 16,000 lbs. The fatigue stress margins are [ ]^{b,c} at the upper core plate/core barrel interface and [ ]^{b,c} at the upper core barrel/core shroud interface.

Table 6-1 Comparison of Calculated RMS Displacements of AP1000 and 3XL

Location	AP1000 RMS Displacement (mils)				3XL RMS Displacement (mils)			
	u_x	u_y	u_3		u_x	u_y	u_3	
USP center	[							] b,c
USP rim								
UCP center								
UCP rim								
CB @ mid-elevation (radial displacement)								
CB–RV								
LCSP rim								
LCSP center								
VSP/LTP								
RV upperhead								
Key-Clevis, Tangential								
CS/CB								
UCP-CB								
CB-RV	[							]

Definitions:
CB = Core barrel
CS = Core shroud
LCSP = Lower core support plate
LTP = Lower tie plate
RV = Reactor vessel
SCS = Secondary core support structures
UCP = Upper core plate
USP = Upper support plate
VSP = Vortex suppression plate
U_x, U_y = Horizontal displacement components
U_z = Vertical displacement

Table 6-2 High Cycle Fatigue Margins to Allowable Values for the Vortex Suppression Plate and Secondary Core Support Structures	
Location	**Margin**
Inner VSP columns	1.9
Outer VSP columns	2.0
Upper section of SCS columns	64.4
Lower section of SCS columns	7.8
Inner VSP column bolts	4.8
Outer VSP column bolts	5.0
Lower section SCS column bolts	15.7

Definitions:
SCS = Secondary core support structures
VSP = Vortex suppression plate

Table 6-3 Comparison of Measured and Calculated Steady Flow Loads

Component	Core Location	Steady Flow Load (lbs)				
		1/7 Scale Model[1]		Doel 3 Hot Functional Test		
		M.[2]	CFD/M.	M.[2]	CFD/M.	CFD Analysis
Guide tube	K-14	[				] b,c
Guide tube	B-8					
Guide tube	H-14					
Support column	M-3					
Support column	B-7	[				]

1. Adjusted to Doel 3 hot functional test conditions
2. M. = Measured

Table 6-4 Calculated Mean Flow Loads

Component	3XL (Doel 3)		AP1000	
	Core Location	Mean Flow Load (lbs)	Core Location	Mean Flow Load (lbs)
Guide tube	K-14	[ ] b,c	B-6	[ ] b,c
Upper support column	M-3	[ ]	B-7	[ ]

Table 6-5 AP1000 Guide Tube High Cycle Fatigue Margins	
Location	**Margin of Safety to ASME Allowable Stresses**
Bottom flange – split tube weld	5.1
Lower guide plate – enclosure pin weld	5.1
Lower guide plate – enclosure pin	0.6
Bottom flange – enclosure weld	27.3
Intermediate flange – enclosure weld	4.6
Support pin, flexible leaf	0.8
Upper and lower guide tube flange bolts	1.9

Table 6-6 Upper Support Column High Cycle Fatigue Margins	
Location	**Margin of Safety to ASME Allowable Stresses**
Base legs	8.0
Base bolts	2.1
Column body/base weld	12.2
Column/top weld	7.7

Table 6-7 Local Flow Turbulence[1] Vibratory Forces on Core Shroud Bolts				
Bolt Number	**Shear-X**	**Shear-Y**	**Shear-Z**	**$(F_x^2 + F_y^2)^{1/2}$**
1	[			] b,c
2				
3				
4				
5				
6				
7				
8				
9				
10				
11				
12				
13				
14				
15				
16				
Sum of forces on all bolts	[			]

1. The vibratory loads due to turbulence excitation of the system fundamental acoustic mode and due to RCP speed-related excitations must still be added in.

Table 6-8 Net Preload Acting on Lower Flange of Core Shroud per Bolt for Hot, Full Power	
Load Source	**Load (lbs)**
Core shroud weight	[ ] b,c
Core shroud buoyancy force	
Hydraulic lift force on the core shroud	
Hydraulic drag force on the core shroud	
Bolt preload	
Net preload	

Table 6-9 Vibratory Forces on AP1000 Core Barrel						
RMS Forces and Moments						
	Axial Force (lbf)	Shear Force (lbf)		Moment (in-lbf)		
		X	Y	X	Y	
Upper support plate flange	[					] b,c
Core barrel flange	[					]

Table 6-10 Summary of Key/Clevis Interface Loads							
	Minimum Clearance (mils)			Peak Interface Load During Time History (lbs)			
Case No.	CB/RV	CB/UCP	CB/CS	CB/RV	CB/UCP	CB/CS	
1	0.1	–	–	[		]	b,c
2	–	0.1	–				
3	–	–	0.1				
4	0.1	0.1	0.1	[		]	

CB = core barrel
CS = core shroud
RV = reactor vessel
UCP = upper core plate

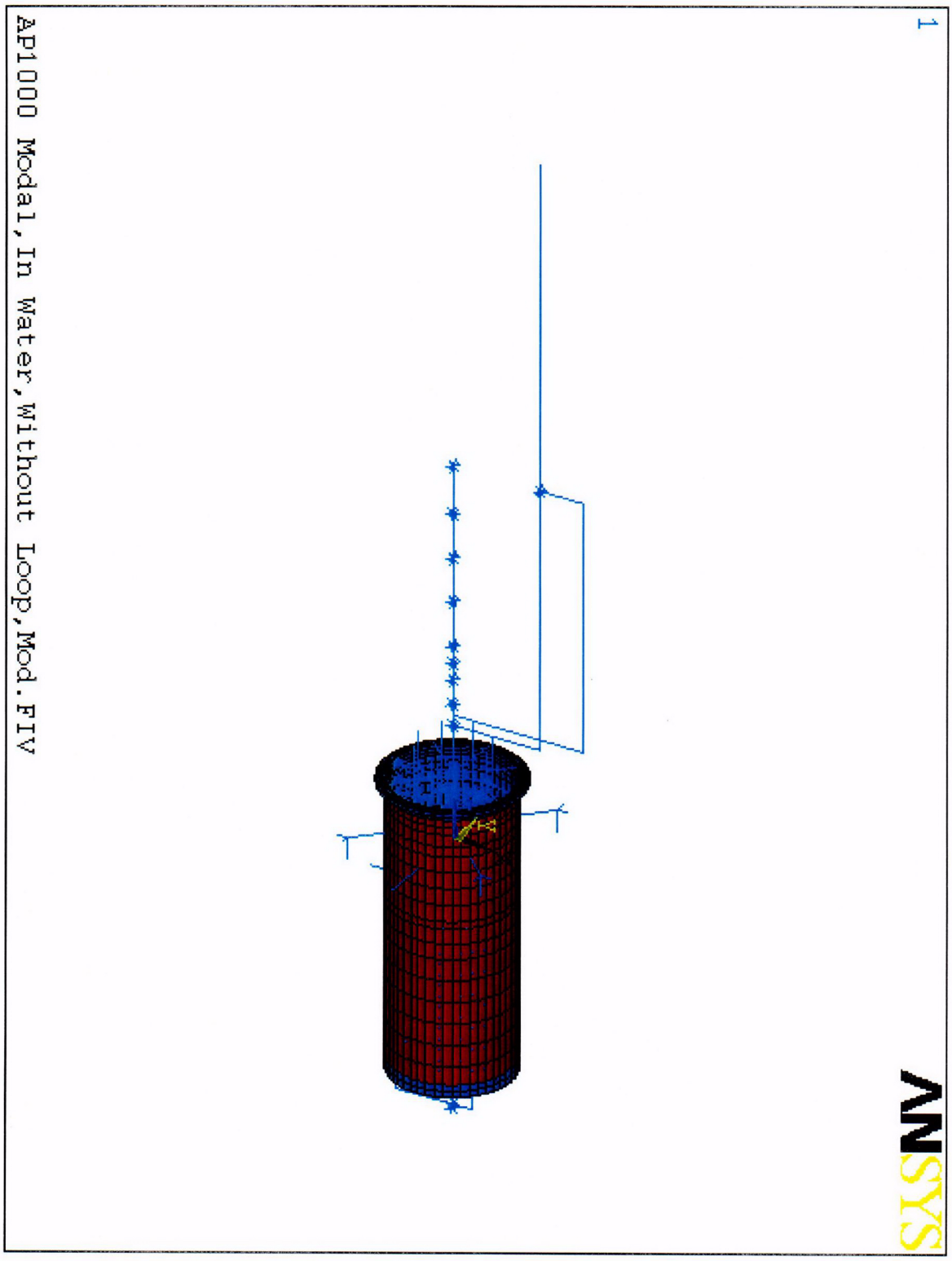

Figure 6-1 AP1000 System Model

C03

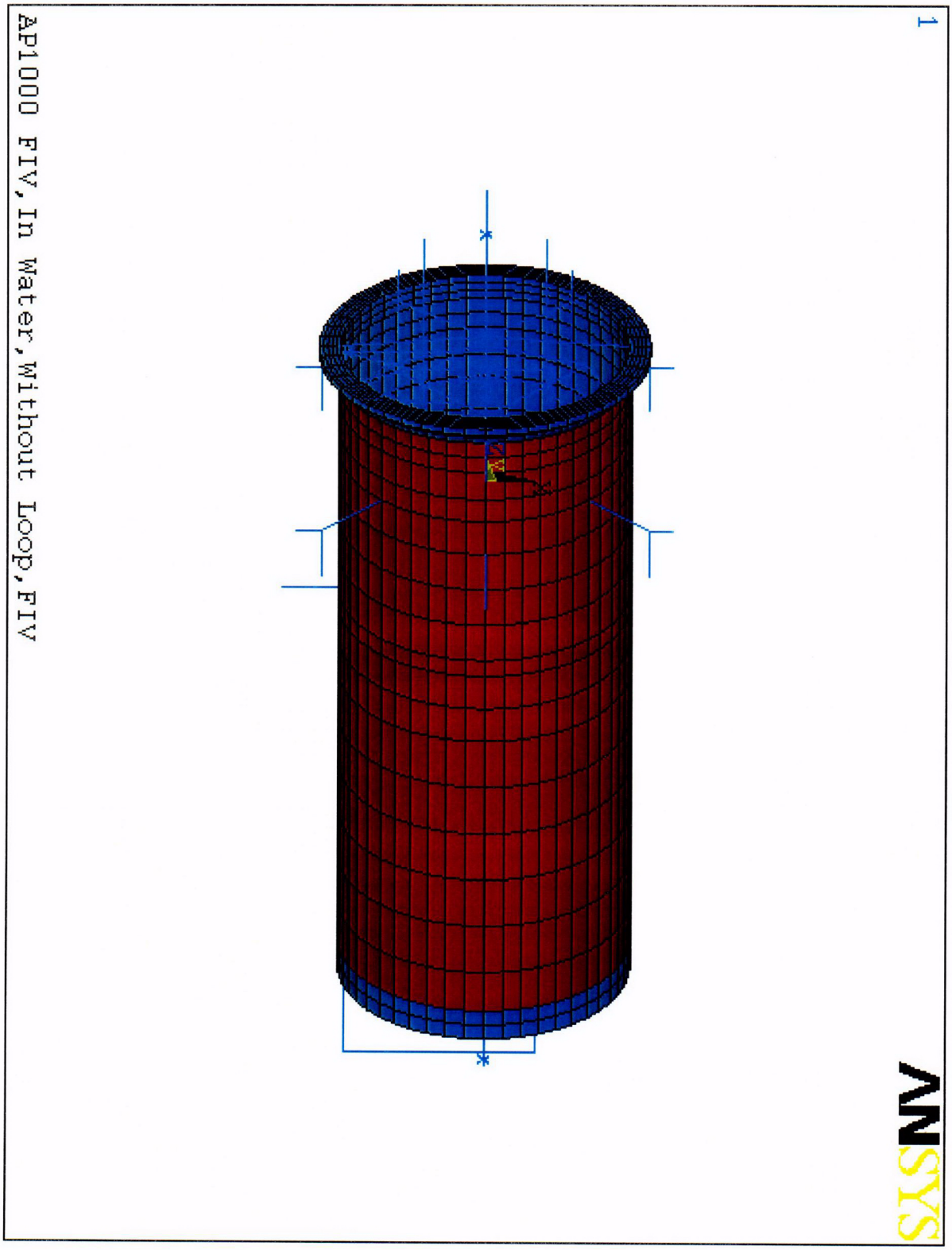

Figure 6-2 Core Barrel for AP1000 System Model

C04

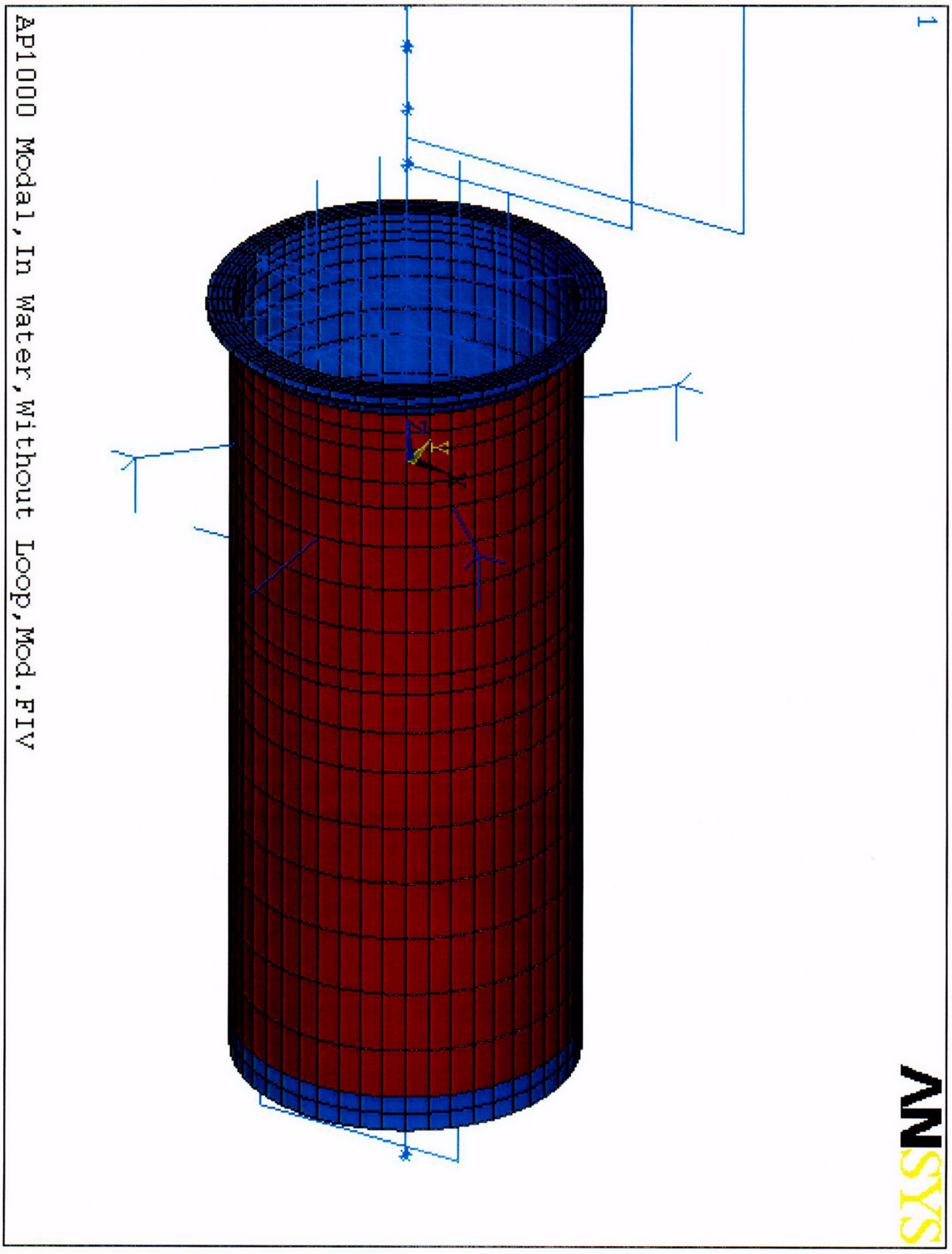

Figure 6-3 AP1000 System Model – Enlarged View

C05

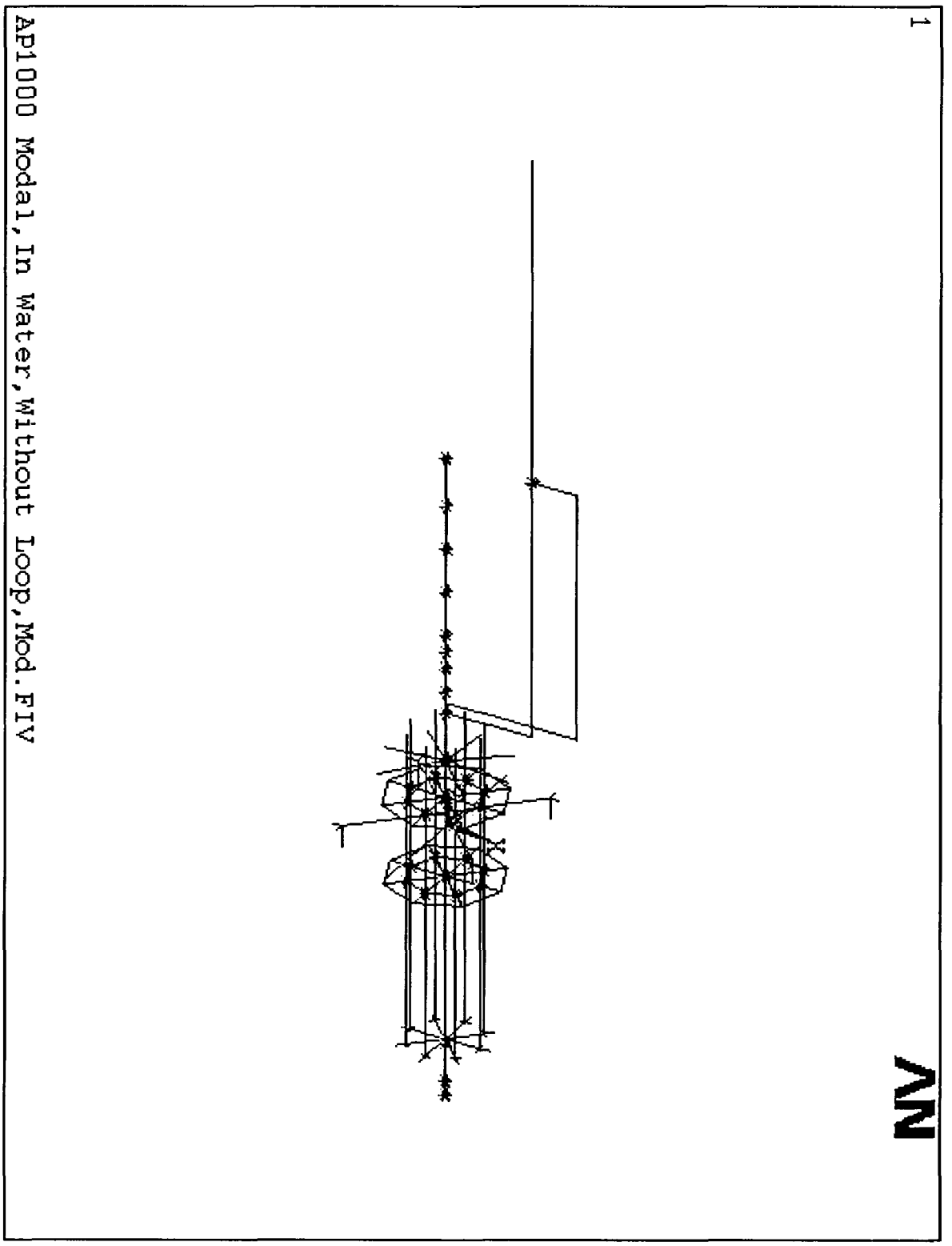

Figure 6-4 AP1000 System Model (Sheet 1 of 3)

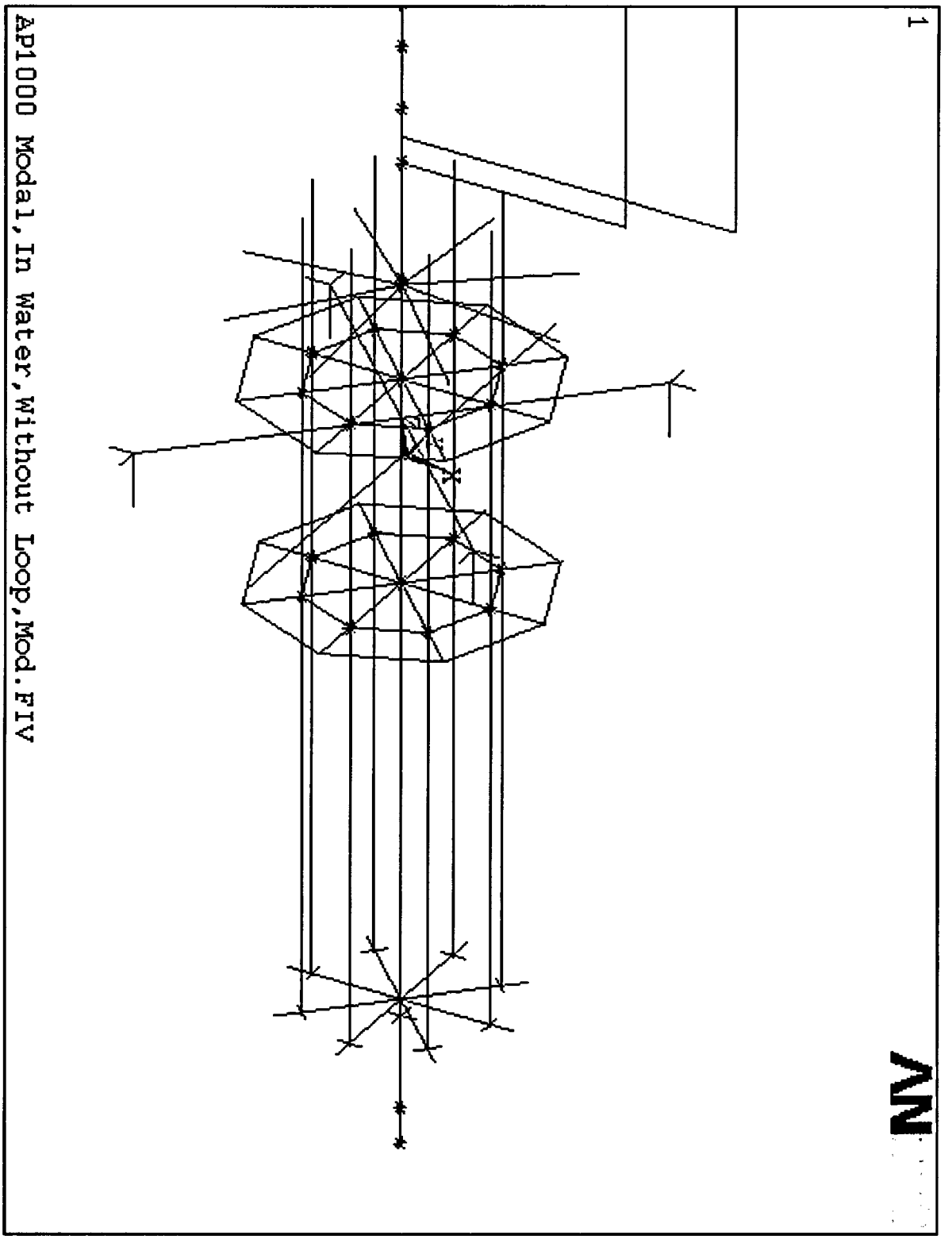

Figure 6-5 AP1000 System Model (Sheet 2 of 3)

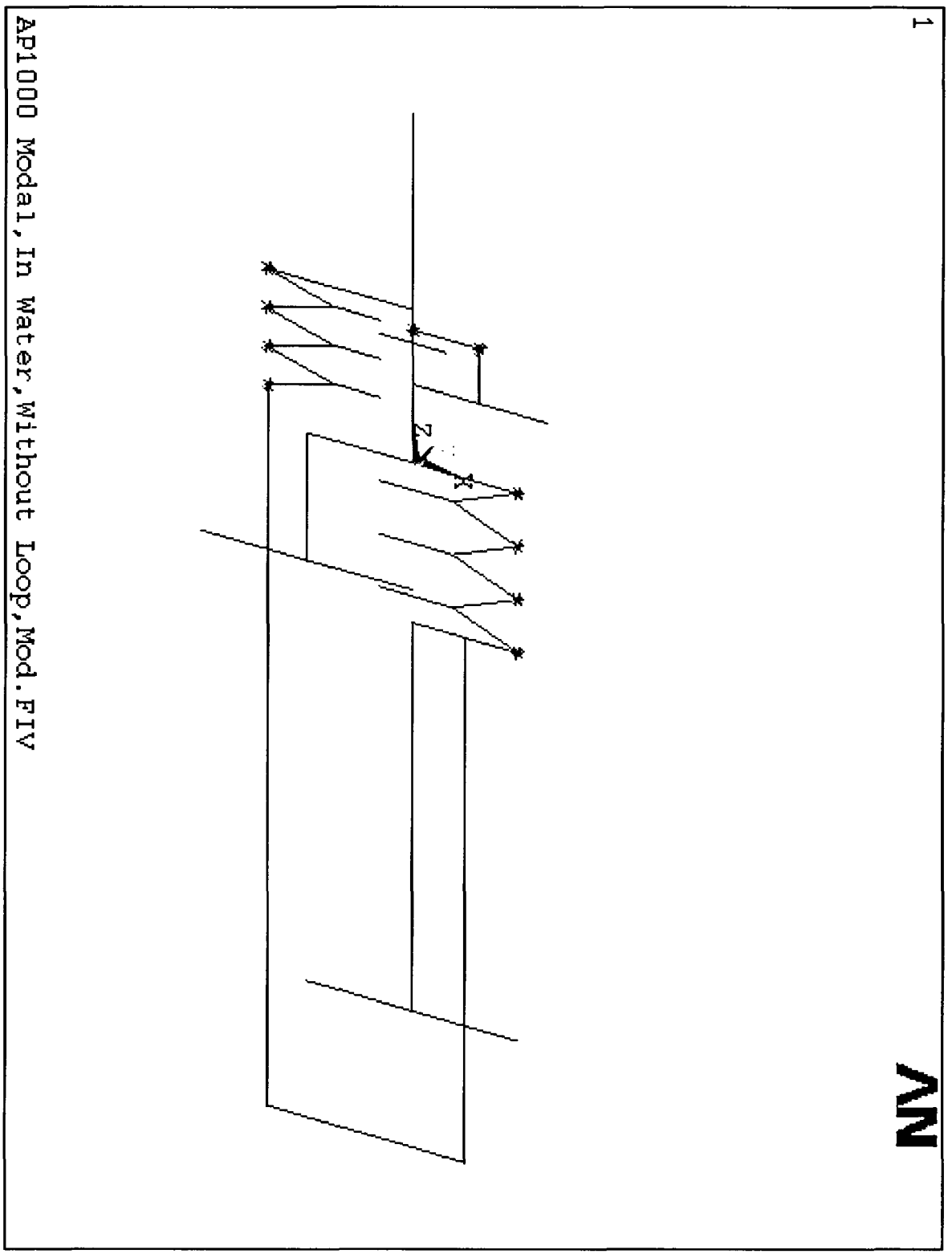

Figure 6-6 AP1000 System Model (Sheet 3 of 3)

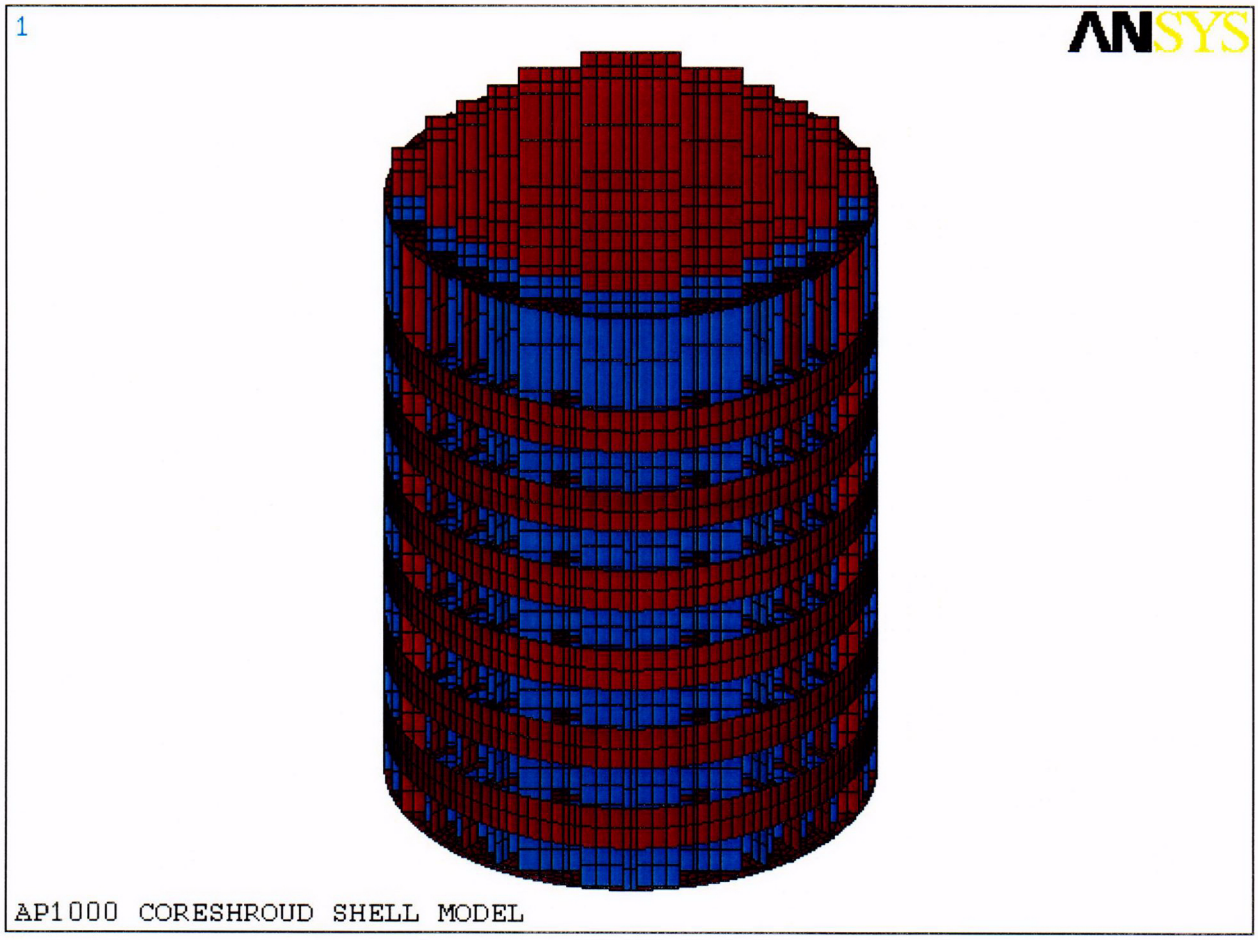

Figure 6-7 Core Shroud Model

C06

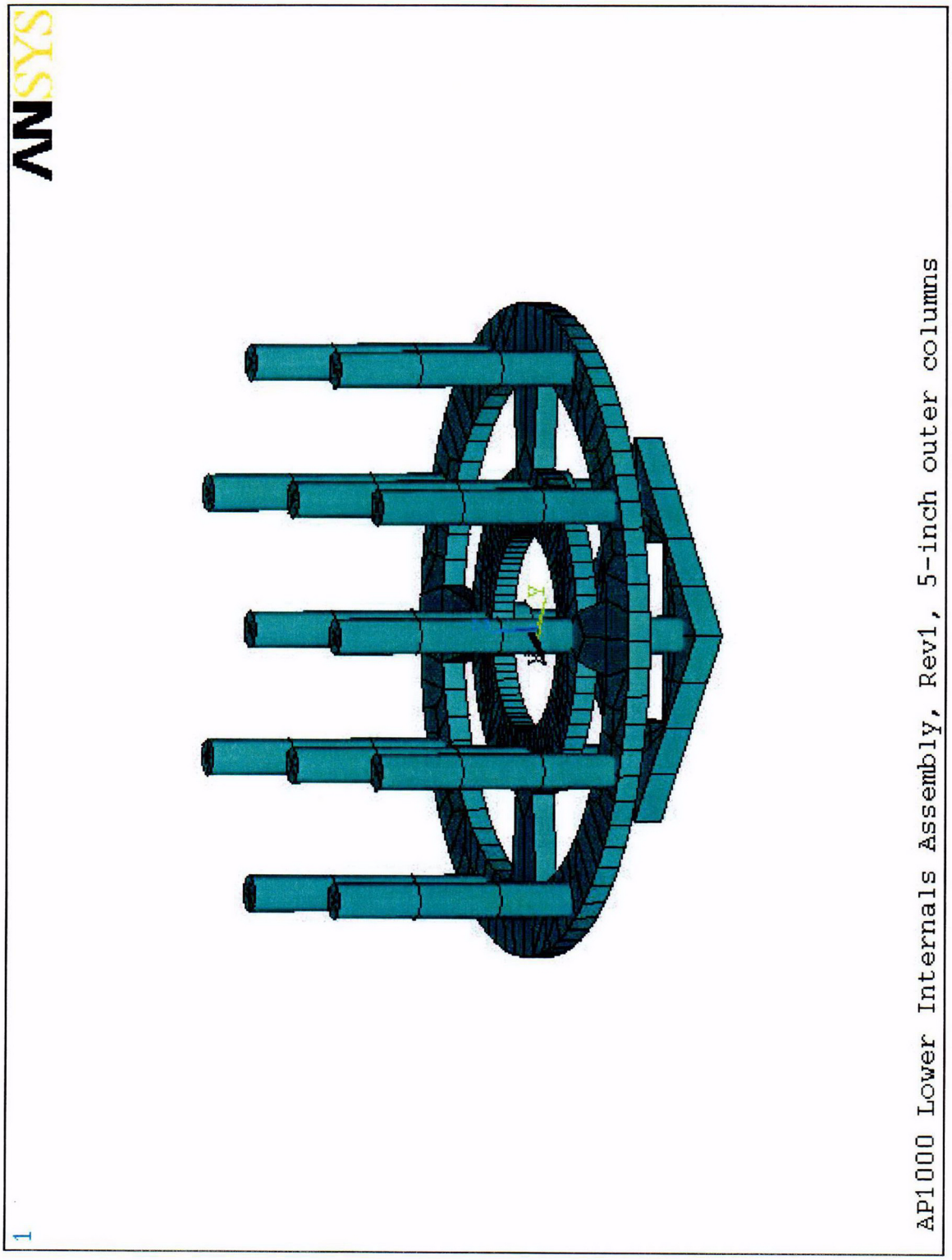

Figure 6-8 Finite Element Model of Vortex Suppression Plate and Secondary Core Support Plate Structures

C07

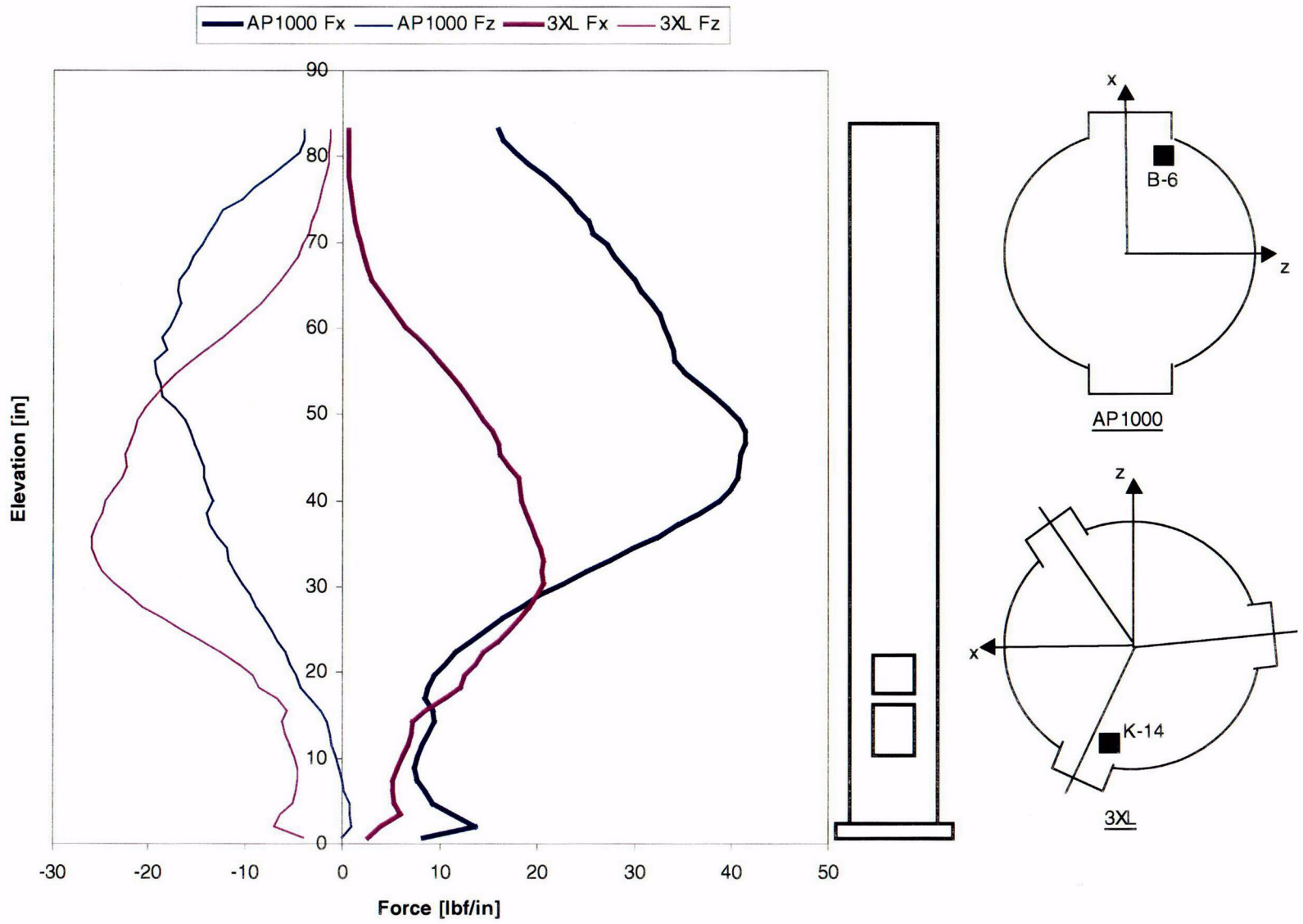

Figure 6-9 Axial Distribution of Mean Flow Load on AP1000 and 3XL Guide Tubes

C08

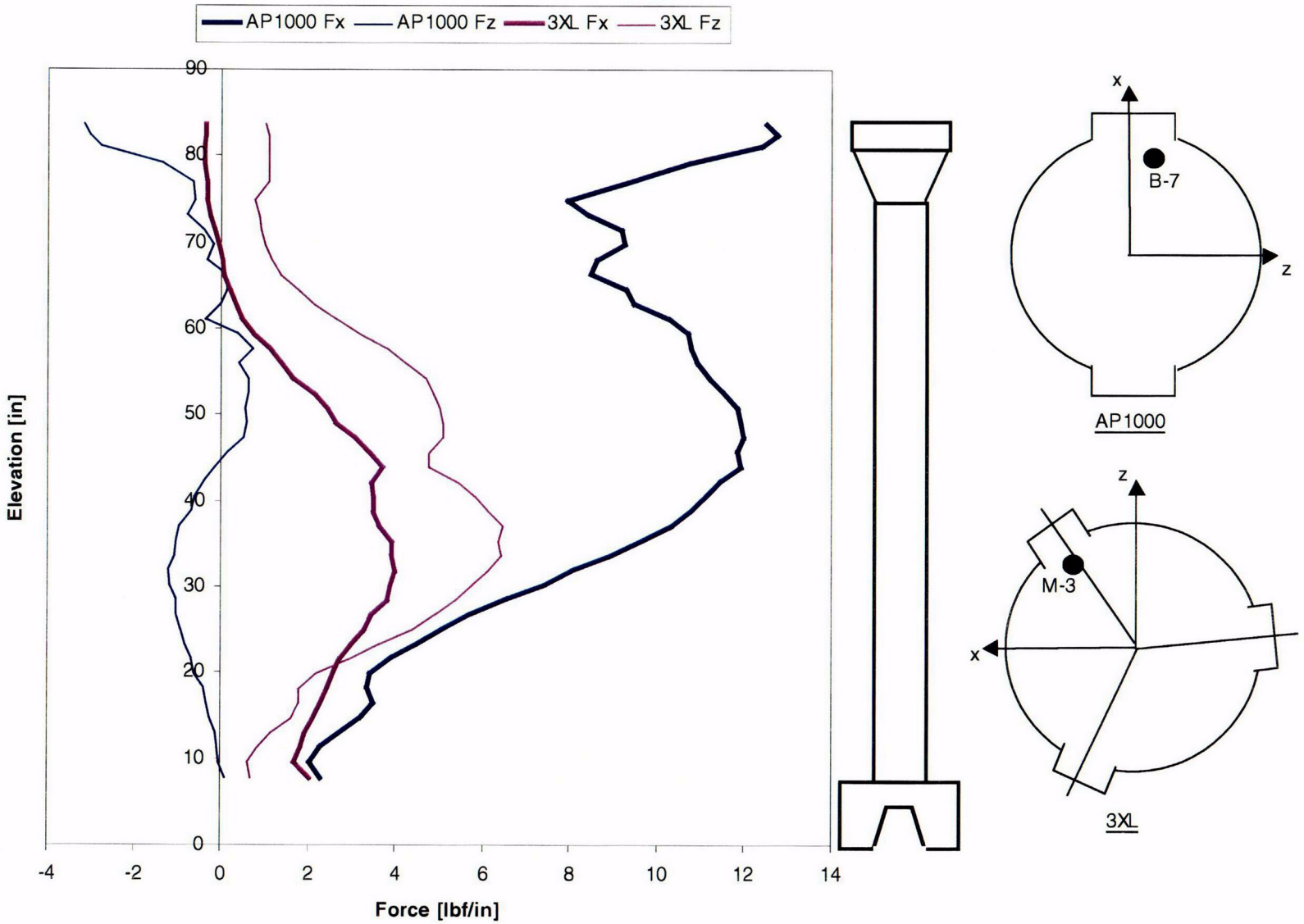

Figure 6-10 Axial Distribution of Mean Flow Load on AP1000 and 3XL Upper Support Columns

C09

7 PREOPERATIONAL INTERNALS VIBRATION MEASUREMENT PROGRAM

Westinghouse is planning a reactor internals flow-induced vibration measurement program during preoperational tests of the first AP1000 plant. This test will be similar to previous plant tests and will provide added assurance of the adequacy of the reactor internals design as part of the vibration assessment program in NRC Regulatory Guide 1.20.

The major structural components of the AP1000 reactor lower internals will be instrumented during preoperational testing. Transducers will be installed on the reactor vessel and the internals before the hot functional test. The integrity of these transducers and the operability of the data acquisition equipment will be verified during this test.

The response of the reactor vessel and the internals due to flow-induced vibration will be measured during the hot functional test. As shown by the results in section 7.8, the dominant vibration modes of the internals with no core present are similar to those with the core in place and their vibration amplitudes are expected to be slightly higher under hot functional test conditions than hot, full-power conditions.

Data will be acquired at several temperatures from cold startup to hot standby conditions. Data will be recorded for pump startup and shutdown transients as well as for all possible combinations of steady-state pump operation. In addition, data will be recorded with none of the pumps operating to determine the background noise level.

Transducer signals will be monitored as they are being recorded to ensure the validity of the data. A spectrum analyzer will be used during the test as an additional check on transducer performance. The spectrum analyzer will also provide preliminary information on the natural frequencies and responses of the instrumented components. The majority of the data, however, will be analyzed from data stored during the test.

The leads for these internally mounted transducers will be routed through the top-mounted instrumentation guide tube conduits. The combined in-core detectors/core exit thermocouples will not be installed during the hot functional test. Special fittings, designed to ASME Section III, Class 1 pressure boundary rules, will be used to seal the transducer leads during this test. These fittings will be removed following the test.

All transducers and associated hardware will be removed after the completion of the hot functional testing.

7.1 LOCATIONS OF TRANSDUCERS

The location and types of transducers to be used for the AP1000 vibration measurement program are shown in Figure 7-1. Detailed transducer locations and their directions of sensitivity are listed in Table 7-1. The measurement objectives for the instrumented components are listed below:

- Four radially sensitive accelerometers mounted near the top of the core shroud. These transducers are to detect shell mode vibration of the core shroud and provide additional information on the core barrel beam modes.

- Two transducers mounted on the upper end of the core shroud to measure the relative vibration displacement between the core barrel and the core shroud.

- Six axially sensitive strain gages mounted just below the core barrel flange. These transducers will detect axial vibration of the lower internals and core barrel beam modes.

- Three axially sensitive strain gages (two inside and one outside) mounted on the upper support assembly skirt to detect vertical motion of the upper support structure. Or alternatively, this information may be obtained using axially sensitive accelerometers.

- Two axially sensitive strain gages located on the outer wall on the core barrel to lower core support plate weld. These strain gages will provide direct information on the stresses at this location, or alternatively, this information may be obtained using axially sensitive accelerometers.

- Four axially sensitive strain gages mounted on two lower support columns that attach the vortex suppression plate to the lower core support plate. These gages will be mounted at 90° separation on two different support columns such that lateral displacement of the vortex suppression plate assembly can be determined. Alternatively, four horizontally sensitive accelerometers will be considered to obtain this information.

- Two axially sensitive strain gages located on the upper support column extension. These transducers will detect the lateral displacement of the extension.

- Four axially sensitive strain gages mounted near the upper end of the most highly loaded upper support column. These transducers will determine beam mode displacement and response frequencies of the upper support column.

- Four vertically sensitive and three horizontally sensitive accelerometers mounted on the reactor head closure studs at 90° intervals. These transducers will detect motion of the reactor vessel and the upper and lower internals flanges.

- Three radially sensitive accelerometers installed on the core barrel at approximately the mid-elevation to determine the shell mode responses of the core barrel.

- Four axially sensitive strain gages installed near the top of the guide tube subjected to the highest flow loads. These transducers will determine the beam mode displacement and response frequencies of the guide tube.

7.2 TRANSDUCERS AND DATA ACQUISITION EQUIPMENT

The strain measurements of the upper support plate skirt, lower core support plate weld, and core barrel flange will use weldable strain gages. These gages have a Ni-Cr filament in a 120 ohm quarter bridge configuration with a nominal gage factor of 1.90. These gages will be temperature-compensated in the range of 75°F to 600°F for mounting on stainless steel. Each gage will be hydrotested by the manufacturer and helium leak-checked upon receipt to verify the integrity of the stainless steel sheath.

The gages will be attached to the component being measured by a number of 5 to 10 watt-second electrical resistance spot welds. The lead wires are fiberglass insulated and enclosed in a stainless steel sheath that protects the leads until they exit the pressure vessel through an instrument penetration. Outside the reactor vessel, the leads will be connected to bridge completion networks containing precision resistors. The strain gage bridges will be located as near to the gage as possible to minimize picking up electrical noise in the gage lead and to minimize gage desensitization. Preamplification will consist of signal conditioning amplifiers, which will provide bridge balancing, shunt calibration, and output filtering.

The internal accelerometers mounted on the lower internals are high temperature and pressure piezoelectric. These transducers will be mounted to the instrumented components by bolts secured by locking devices. These uniaxial accelerometers will be supplied with integral leads of sufficient length to exit the reactor vessel via the head penetrations.

In addition, uniaxial sensitive piezoelectric accelerometers will be mounted on the reactor vessel head studs to measure horizontal and vertical movement. Short lengths of high-temperature, low-noise cable will extend the leads through the vessel insulation.

Both the internally and externally installed accelerometers will use fixed gain remote charge amplifiers that result in output in voltage. Power for these remote charge amplifiers will be provided by signal conditioners located near the recording equipment.

The accelerometers will be checked with a vibration shaker, which provides a known acceleration level. This acceleration level will be applied to the accelerometer near its installation location and read out on the data acquisition equipment. This will act as a check on the amplifiers as well as on the accelerometers themselves.

The internally mounted transducers will have their leads protected from impinging flow using methods from previous Westinghouse plant tests. The leads from the transducers installed on the lower internals will be shielded from flow by protective covers similar to ones used at Doel 4.

The output from the strain gage and accelerometer signal conditioners will be routed to a switching panel. Selected signals will then be further amplified and filtered by differential DC amplifiers (or equivalent) before being recorded. Both the input and output signals will be monitored with a dual-channel

oscilloscope to ensure data are being properly recorded without saturation and with the optimum signal-to-noise ratio.

The data will be suitably recorded to cover the 0 to 1000 Hz frequency band of interest. Recordings for steady pump operation will be 10 to 20 minutes long to allow for proper signal averaging in later analysis. For each data record, the time, tape number, tape position, recording parameters, signal conditioner parameters, and pertinent reactor and test conditions will be recorded on log sheets. Onsite analysis will consist mainly of using a real-time spectrum analyzer to generate linear voltage spectra.

7.3 EQUIPMENT CALIBRATION

The procedure to be used to ensure that all equipment is calibrated and properly functioning is as follows. Before shipment of the equipment to the plant site, all instrumentation will be calibrated and certified by Westinghouse or by a suitable calibration laboratory with the National Institute of Standards and Technology (NIST) traceability. Upon arrival at the site, the instruments will be checked with a reference voltmeter to verify that all Westinghouse measurement equipment is functional.

At the beginning of each data record, a reference 1-volt RMS 100 Hz sine wave will be inserted through the amplifiers and recorded on each data channel. This signal will be used to adjust the playback electronics during subsequent data analysis. Also recorded will be signal outputs of the strain measuring system when a strain response is simulated by use of the shunt resistors in the strain gage signal conditioners. A random noise signal consisting of white noise will also be recorded on the first data record to check the interchannel phase relationship.

At completion of the data collection program, the measurement instruments will again be rechecked by comparing the equipment output signals to known input reference voltages.

7.4 DATA REDUCTION

The techniques used to reduce the signals will include generation of time histories using a recording oscillograph, and preparation of linear frequency spectra using a real time fast fourier transform analyzer. The plotted spectra will be used to determine the predominant responses and their associated frequencies. The time histories will be used to determine the change in mean response levels due to pump startup and shutdown transients.

7.5 HOT FUNCTIONAL TEST CONDITIONS

Flow-induced vibration data will be acquired during the hot functional test. Data will be recorded at several temperature plateaus corresponding to the plant startup pre-operational test requirements. These measurements will indicate the variation in response due to temperature changes from cold startup to hot standby conditions. Maximum levels are expected to occur at 200° to 250°F. The levels in this temperature band are expected to be [ ]^{bc} percent greater than the hot, full-power levels. Most of the data will be recorded near the hot standby temperature of 529°F and will include pump transients as well as all possible combinations of steady-state pump operation.

The pump operating modes at which data will be recorded include:

- No pumps operating – records made of background noise.
- Startup transients – to record mean strains and transient vibration behavior that results from pump startup.
- Steady operation of one or more pumps – to identify vibration response of instrumented components during various flow conditions.
- Shutdown transients – flow-induced mean strains and transient vibration behavior are deduced from these records by noting the change in strain levels through the pump transient.

A simultaneous shutdown of all four pumps may also be conducted to provide a direct measurement of the mean strains between full-flow and zero-flow conditions.

The reactor internals will be subjected to higher flow loads during the Hot Functional Test than for normal operation with the core installed. Vibration levels are generally lower with the addition of the core than for the hot functional testing (References 1-7 and 7-1). Therefore, the responses measured during the hot functional test will be conservative with respect to normal operating conditions.

7.6 PREDICTED RESPONSES

The predicted responses will be established at a later date and will be used to determine the expected responses at the appropriate transducer locations along with corresponding acceptable values. The results of previous scale model and full-scale plant tests may be incorporated in this analysis. Acceptable vibratory responses will be based on the allowable fatigue stress values in Figures I-9.0 of the ASME Boiler and Pressure Vessel Code, Section III, Division I Appendices, 1998 Edition with 2000 Addenda.

7.7 COMPARISON OF CALCULATED HOT FUNCTIONAL TEST RESPONSES TO RESPONSES CALCULATED FOR HOT, FULL-POWER CONDITION

7.7.1 Flow Turbulence Induced Vibration

Modal analyses of the AP-1000 reactor were run both with and without the fuel assemblies to represent the normal operation and hot functional test plant conditions, respectively.

The flow rates are approximately [ ]^{bc} gpm at hot, full-power with core and [ ]^{bc} gpm during the hot functional test.

The mode shapes from the AP1000 system model for hot, full-power and the hot functional test are compared in Figure 7-2 (core barrel beam modes) and Figure 7-3 (core shroud beam modes). These analytical results indicate similar frequency responses (see Table 7-2) and mode shapes with and without the core. Similar behavior has also been demonstrated in plant vibration test programs conducted at Trojan 1 and Sequoyah 1 during hot functional and initial startup testing.

As discussed previously, comparison of the beam mode shapes indicates that the basic behavior is the same for the two conditions. In addition, the higher inlet flow rate of the hot functional test indicates that the flow turbulence induced vibrations of the lower internals will be greater than those at the hot, full-power condition.

For the components of the upper internals, guide tubes, and support columns, the values of the product of the fluid density and the flow velocity raised to a power of two, ρV^2, will be similar for the two conditions if a debris filter is installed for hot functional testing. This occurs because the effects of the core outlet temperature at full power on fluid density and, therefore, velocity offset the higher inlet flow velocity of the hot functional condition. With two pumps on one side of the reactor in operation and the other two off, the flow velocities past the guide tubes in front of the active loop outlet nozzle will be greater than those at the hot, full-power condition.

7.7.2 Reactor Coolant Pump Induced Vibrations

RCP-induced stresses are a small part of the total, and therefore, should not be a major influence regarding the conservatism of the hot functional test.

7.8 TEST PROGRAM SUMMARY

The adequacy of the internals design with respect to flow-induced vibration will be confirmed by the visual pre- and post-hot functional inspections. At the completion of the hot functional test, the internals will have been subjected to more than 240 hours of greater than normal full-flow conditions. Additional time will have been accumulated with one, two, or three pumps in operation. This results in more than one million cycles of vibration for the major structural components.

The AP1000 vibration measurement program will determine the natural frequencies, modes, and amplitudes of the major structural components due to flow-induced vibration. These measured responses will serve as an additional technical basis to the vibration assessment program and previous plant and scale model tests.

All the transducers and associated hardware will be removed after the completion of the hot functional test before core loading. The special pressure boundary fittings at the top of the in-core instrumentation conduits will also be removed.

Table 7-1 AP1000 Transducer Locations

Instrumented Component	Number and Type of Transducers	Transducer Locations	Direction of Sensitivity
Core shroud (inner wall)	4 accelerometers	0°, 180°, 225°, 270°	Radial
Core shroud to core barrel	2 relative displacement transducers	0°	Radial
Core barrel flange (outer wall)	4 strain gages	0°, 90°, 180°, 270°	Axial
Core barrel flange (inner wall)	2 strain gages	180°, 270°	Axial
Core barrel mid-elevation	3 accelerometers	0°, 180°, 225°	Radial
Core barrel mid-elevation	1 pressure transducer	0°	Radial
Upper support skirt (Inside and outside)	3 strain gages	180°, 90° inside 90° outside	Axial
Lower core support plate weld (outside)	2 strain gages	0°, 90°	Vertical
Vortex suppression plate support columns (2)	4 strain gages or 4 accelerometers	On column nears LCSP or on vortex suppress ring	Axial Horizontal
Reactor vessel (head studs)	4 accelerometers 3 accelerometers	0°, 90°, 180°, 270° 0°, 90°, 180°	Vertical Horizontal
Support column extension	2 strain gages	0°, 90°	Axial
Guide tube	4 strain gages	0°, 90°, 180°, 270°	Axial
Upper support column	4 strain gages	0°, 90°, 180°, 270°	Axial
Total number of transducers	35 7	Internal (reactor internals) External (reactor vessel)	

Table 7-2 AP1000 Natural Frequencies – With and Without Core (Hz)		
	AP1000 (With Core)	**AP1000 (Without Core)**
Fuel assembly First beam mode	[	] b,c
Core barrel Cantilever beam mode n = 2 shell mode n = 3 shell mode		
Core shroud Cantilever beam mode n = 2 shell mode n = 3 shell mode		
Reactor vessel Rocking beam mode Translation mode		
Vertical modes Upper internals Lower internals	[	]

1. Core barrel and core shroud coupled
2. Includes water participation

N/A = not applicable

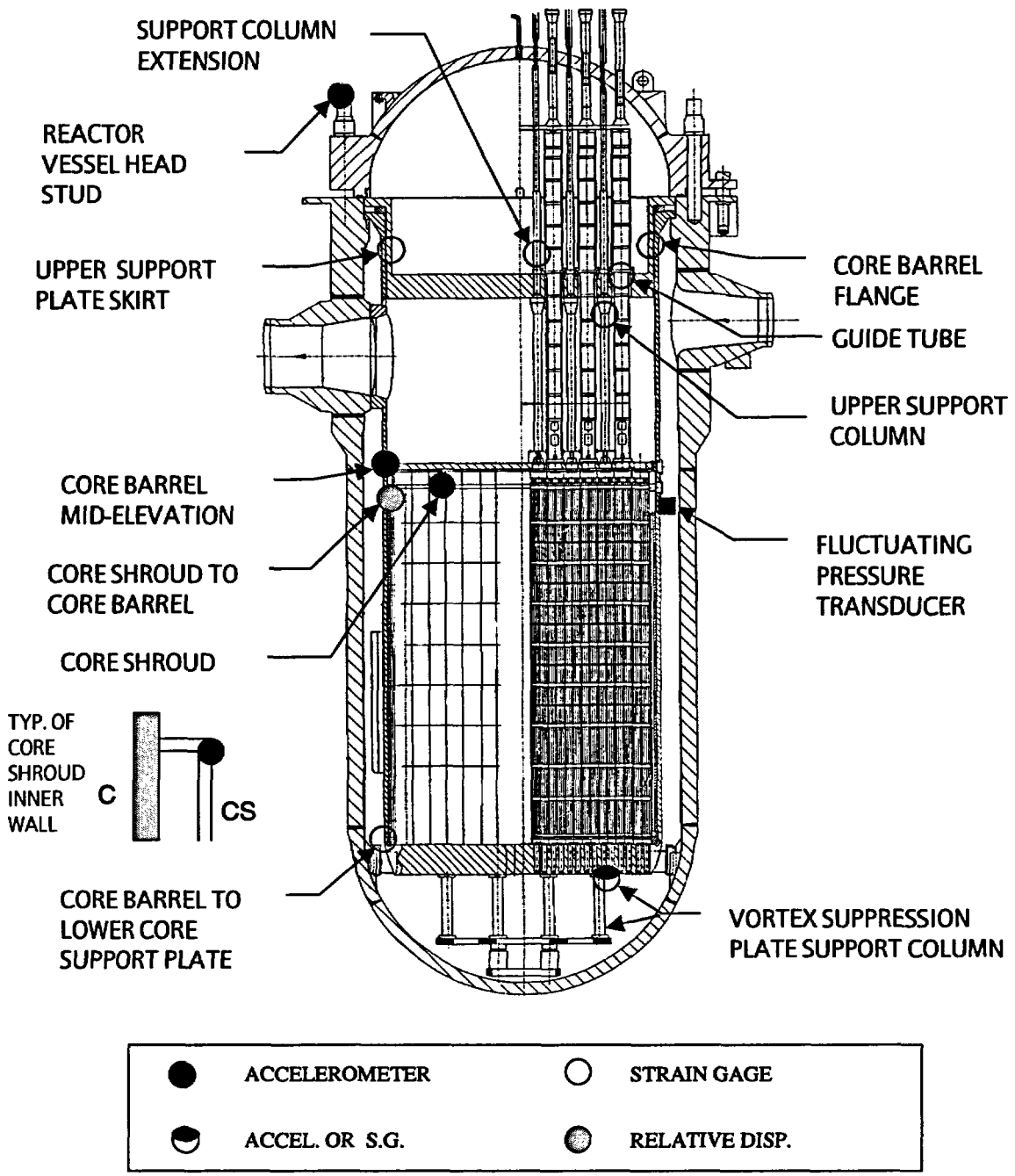

Figure 7-1 Location of Transducers for AP1000 Preoperational Vibration Measurement Program

b,c

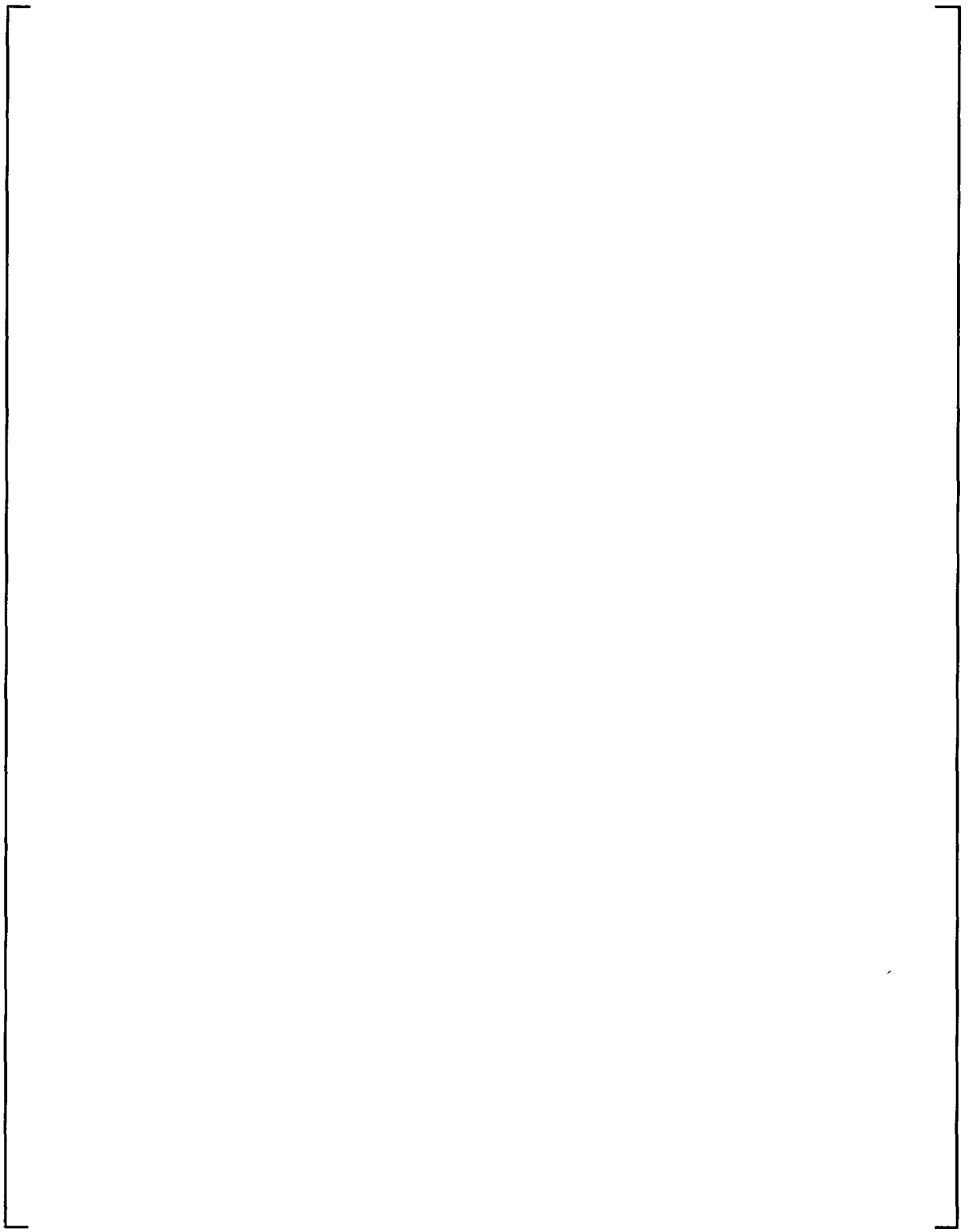

Figure 7-2 Core Barrel Beam Mode Shapes for AP1000 With and Without Core

b,c

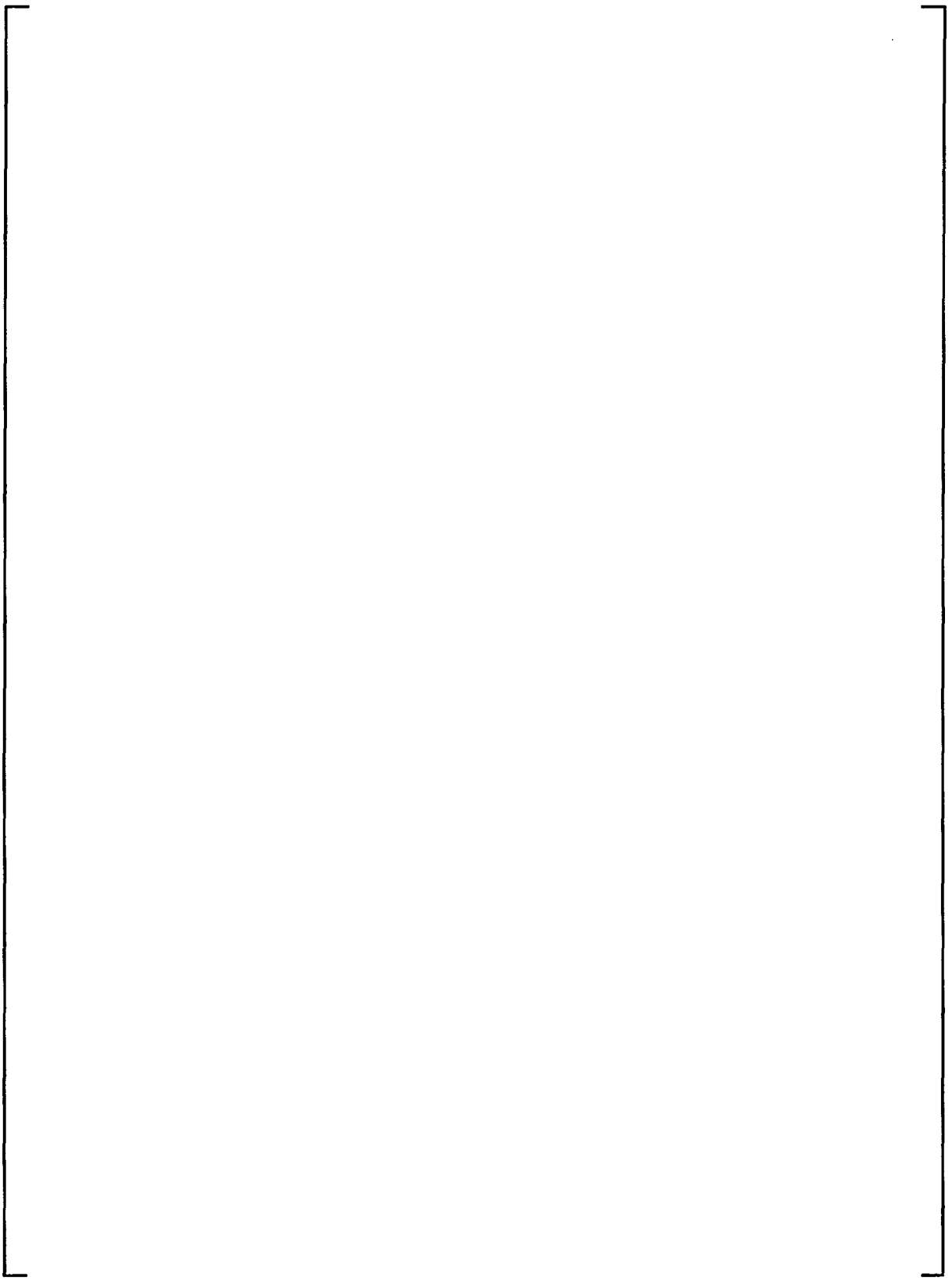

Figure 7-3 Core Shroud Beam Modes With and Without Core

8 PRE- AND POST-HOT FUNCTIONAL INSPECTION

The Westinghouse three-loop Internals Assurance Program (Reference 1-3) includes visual examinations of the reactor vessel and internals before and after the completion of the hot functional test. The internals are removed from the reactor vessel, and the following areas are inspected under 5X or 10X magnification:

- All major load-bearing elements of the reactor internals relied upon to retain the core support structure in position
- The lateral, vertical, and torsional restraints provided within the vessel
- Those locking and bolting components whose failure could adversely affect the structural integrity of the reactor internals
- Those surfaces known to be, or may become, contact surfaces during operation
- Those critical locations on the reactor internal components as identified by the vibration analysis
- The interior of the reactor vessel for evidence of loose parts or foreign material

The results of these inspections will be recorded on the AP1000 Vibrational Check-Out Functional Test Inspection Data drawing.

Acceptance standards are the same as required in the shop by the original design drawings and specifications.

During the hot functional test, the internals will be subjected to a total operating time at greater than normal full-flow conditions (four pumps operating) of at least 240 hours. This provides a cyclic loading of approximately one million cycles on the main structural elements of the internals. In addition, there will be some operating time with one, two, and three pumps operating.

When no signs of abnormal wear, no harmful vibrations are detected, or no apparent structural changes take place, the AP1000 reactor internals are considered to be structurally adequate and sound for operations.

9 CONCLUSIONS

Westinghouse has performed analyses of the AP1000 reactor vessel and internals to assess the internal vibration levels expected during plant operation. Westinghouse has developed analytical models of reactor designs similar to the AP1000, which have previously completed reactor internal vibration measurement programs and scale model tests. Westinghouse has benchmarked the analytical models against these past tests, and has applied these analytical techniques to the AP1000 analysis. The AP1000 analyses benchmarked to scale model tests and the instrumented plant tests show that the internals vibration levels are acceptable and that the AP1000 reactor internals design is adequate to ensure structural integrity against flow-induced vibrations.

The recommendations of NRC Regulatory Guide 1.20 are satisfied by conducting the confirmatory pre- and post-hot functional visual and nondestructive surface examinations and the limited measurement program on the AP1000 prototype plant. The plant preoperational test program and the pre- and post-hot functional test examinations are described in sections 7 and 8, respectively.

10 REFERENCES

1-1 "Regulatory Guide 1.20 – Reactor Internals Vibrations Assurance," Nuclear Safety Position Paper No. RG-1.20 R0, Revision 0, 1/8/75.

1-2 "Regulatory Guide 1.20, Revision 2, May 1976," "Comprehensive Vibration Assessment Program for Reactor Internals During Preoperational and Initial Startup Testing," Nuclear Safety Position Paper No. RG-1.20 R1, RG-1.20 R2, Revision 1, July 1976.

1-3 Kuenzel, A. J., "Westinghouse PWR Internals Vibrations Summary 3-Loop Internals Assurance," WCAP-7765-AR (November 1973).

1-4 "AP600 Reactor Internals Flow-Induced Vibration Assessment Program," WCAP-14761, March 1996.

1-5 Boyd, C. H., Ciaramitaro, W. R., and Singleton, N. R., "Verification of Neutron Pad and 17x17 Guide Tube Designs by Pre-Operational Tests on Trojan Power Plant," WCAP-8766 (Proprietary) and WCAP-8780 (Non-Proprietary), May 1976.

1-6 Lee, H., "Prediction of the Flow-Induced Vibration of Reactor Internals by Scale Model Tests," WCAP-8303-P-A (Proprietary) and WCAP-8317-A (Non-Proprietary), July 1975.

1-7 Boyd, C. H. and Singleton, N. R., "UHI Plant Internals Vibration Measurements Program and Pre- And Post-Hot Functional Examinations," WCAP-8516-P (Proprietary) and WCAP-8517 (Non-Proprietary), March 1975.

1-8 Altman, D. A., et al., "Verification of Upper Head Injection Reactor Vessel Internals by Pre-Operational Tests on Sequoyah-1 Power Plant," WCAP-9944 (Proprietary) and WCAP-9954 (Non-Proprietary), July 1981.

1-9 "Mesures Vibratoires Sur Les Equipements Internes De Cuve De Doel 3," EEP-DC-0336, Framatome Document.

1-10 Abou-Jaoude, K. F. and Nitkiewicz, J. S., "Doel 4 Reactor Internals Flow Induced Vibration Measurement Program Final Report," WCAP-10846, March 1985.

3-1 "Mesures Vibratoires Sur Les Equipements Internes De Cuve De Paluel-1," EEP-DC-0458, Framatome Document.

3-2 T. D. Radcliff, W. S. Johnson, J. R. Parsons, Visualization and Control of Vortical Flow in the Lower Plenum of the Westinghouse AP600 Reactor, Univ. of Tenn., April 1993.

4-1 "Vibration Measurements on the Tricastin 1 R. V. Internals," Rpt. No. 873 TN 17106.

4-2 D. E. Boyle, "RGE Mechanical Vibration Measurements," WCAP 7556, August 1970.

5-1 R. D. Blevins, "Flow-Induced Vibration," Van Nostrand Reinhold, 1990, pg. 265.

5-2 L. A. Shockling and N. R. Singleton, "WCAP-9644, 3XL 1/7 Scale Model Internal Flow Test: Structural Response Report," March 1983.

5-3 AEA Technology Engineering Software Limited, CFX-5 User Documentation, Discot Oxfordshire, United Kingdom, 2001.

5-4 Au-Yang, M. K. and Jordan, K. B., "Dynamic Pressure Inside a PWR – A Study Based on Laboratory and Field Test Data," Nuclear Engineering and Design 58, 1980, pp. 113-125.

5-5 ACSTIC COMPUTER CODE, An Acoustic Harmonic Analysis Program for Evaluating the Effects of Periodic, Fluid Borne Pulsations in Fluid-Handling Systems.

5-6 R. E. Schwirian et al., "A Method for Predicting Pump-Induced Acoustic Pressures in Fluid-Handling Systems," PVP-Vol. 63 (ASME), pp. 167-184.

5-7 WCAP-10239, "Pump Induced Acoustic Pressure Differentials On Guide Tubes and Support Columns: Experiment and Analysis," January 1983, Westinghouse Proprietary Class 1.

5-8 K. F. Abou-Jaoude and J. S. Nitkiewicz, "Doel 4 Reactor Internals Flow-induced Vibration Measurement Program," WCAP-10846, March 1985.

6-1 P. R. Assedo, P. Bolle, and E. Dubreux, "Mesures Vibratories Sur Les Equipements Internes De Cuve De Doel 3," March 17, 1982.

6-2 WCAP-10322, Revision 1, "Stress Report of 312 Standard Reactor Core Support Structures and Fatigue Analysis," Volume 4.

6-3 H. J. Connors, "Fluidelastic Vibration of Heat Exchanger Tube Arrays," Westinghouse Research Report 77-1E7-FLVIT-P1, March 1, 1977.

7-1 Singleton, N. R., Altman, D. A., and Ciaramitaro, W. R., "Trojan Unit 1 Initial Startup and Hot Functional Vibration Measurements," WCAP-9115 (Proprietary), June 1977.